

Vertebrate Paleobiology and Paleoanthropology Series



Christian F. Kammerer  
Kenneth D. Angielczyk  
Jörg Fröbisch *Editors*

# Early Evolutionary History of the Synapsida

# Chapter 13

## New Material of *Microgomphodon oligocynus* (Eutherapsida, Therocephalia) and the Taxonomy of Southern African Bauriidae

Fernando Abdala, Tea Jashashvili, Bruce S. Rubidge, and Juri van den Heever

**Abstract** An exceptionally well-preserved specimen of the bauriid therocephalian *Microgomphodon oligocynus* from the Burgersdorp Formation (Early-Middle Triassic, *Cynognathus* Assemblage Zone) of the South African Karoo is described. In addition, a taxonomic revision of bauriid therocephalians from southern Africa, based on firsthand examination of almost all known specimens, is presented. *Microgomphodon oligocynus* and *Bauria cynops* are recognized as the only valid species of southern African bauriids. *Microgomphodon oligocynus* is differentiated from *B. cynops* on the basis of clear-cut morphological features such as the presence of a complete postorbital bar, pineal foramen, contribution of the vomer to the osseous secondary palate, comparatively large orbits, presence of a lateral fossa on the posterior portion of the horizontal ramus and on the coronoid process of the dentary, and reduced number of postcanines. Procrustes analysis of the two best-preserved

specimens of these species allowed recognition of further shape differences: *M. oligocynus* has a taller but narrower cranium, taller snout, temporal opening more expanded laterally, pterygoid process located more anteriorly, and smaller suborbital vacuity. The mandible of *M. oligocynus* has a higher symphysis, relatively short corpus, and more laterally-directed coronoid process. *Microgomphodon oligocynus* is known from the Olenekian to what are probably late Anisian levels in South Africa and Namibia, whereas *B. cynops* is restricted to the early Anisian of South Africa.

**Keywords** Karoo • Namibia • Theriodontia • Triassic • Procrustes analysis

### Introduction

Therocephalians are a morphologically varied group of advanced therapsids that are well-represented in the Permian-Triassic South African Karoo Basin. This group was taxonomically very diverse during the Late Permian but became less varied in the Triassic, with ~30 genera in the South African Late Permian and only 10 from the Triassic *Lystrosaurus* and *Cynognathus* assemblage zones (LAZ and CAZ, respectively). Currently there is discussion as to the monophyly of the Therocephalia. Abdala (2007) and Botha et al. (2007) proposed that the taxon was paraphyletic, as *Theriognathus* was found to be the sister group of cynodonts and basal therocephalians such as Lycosuchidae and Scylacosauridae were recovered outside of the group consisting of all other therocephalians. Conversely, Huttenlocker (2009), using a large data matrix and more therocephalian terminal taxa, found the group to be monophyletic as previously proposed by Hopson and Barghusen (1986).

Bauriids from the CAZ were the last surviving therocephalians. Originally they were included among cynodonts (Broom 1911, 1913) as they share several common features (e.g., similar number of upper and lower incisors and the

---

F. Abdala (✉) · B. S. Rubidge  
Evolutionary Studies Institute, University of the Witwatersrand,  
Private Bag 3, Wits, Johannesburg 2050, South Africa  
e-mail: nestor.abdala@wits.ac.za

B. S. Rubidge  
e-mail: bruce.rubidge@wits.ac.za

T. Jashashvili  
Institute for Human Evolution, University of the Witwatersrand,  
Private Bag 3, Wits, Johannesburg 2050, South Africa  
e-mail: tjashashvili@yahoo.fr

and  
Anthropological Institute and Museum, University of Zurich,  
8057 Zurich, Switzerland

and  
Department of Geology and Paleontology, Georgian National  
Museum, 0105 Tbilisi, Georgia

J. van den Heever  
Department of Botany and Zoology, University of Stellenbosch,  
Private Bag X1, Matieland 7602, South Africa  
e-mail: javdh@maties.sun.ac.za

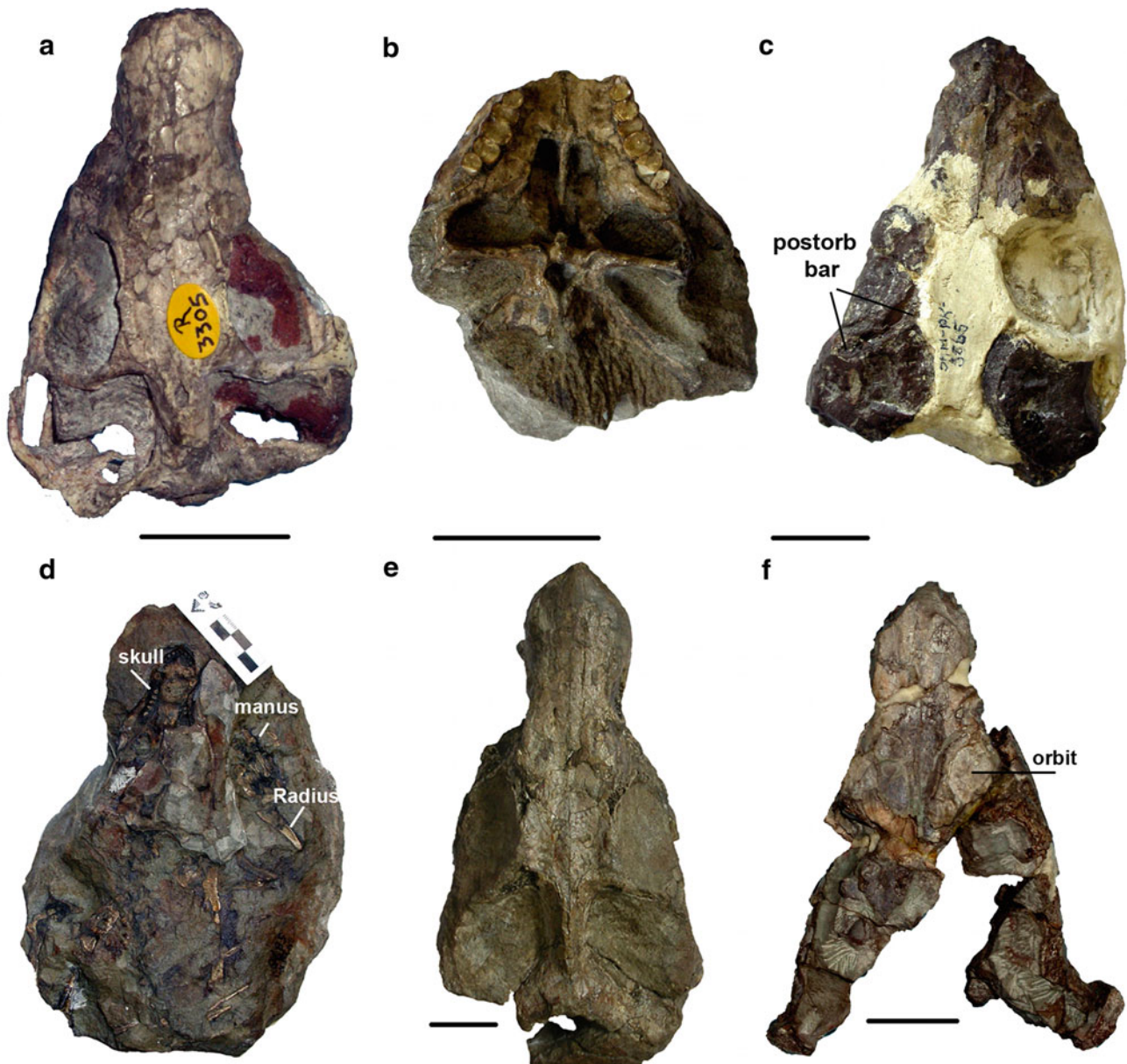


**Fig. 13.1** Holotypes of bauriid species: **a** dorsal view of the skull of *Microgomphodon oligocynus*; **b** ventral view of the skull of *Melinodon simus*; **c** dorsal view of the skull of *Sesamodon browni*; **d** view of the block with skull and partial postcranium of *Aelurosuchus browni*; **e** dorsal view of the skull of *Bauria cynops*; **f** dorsal view of the skull

of *Baurioides watsoni*; **g** dorsal view of the skull of *Watsoniella breviceps*; **h** block showing the partial skull and mandible, partial mandible and partial skeleton (right side) of *Sesamodontoides pauli*; **i** dorsal view of snout of *Bauria robusta*; **j** dorsal view of *Herpetogale marsupialis*. Scale bar in all figures except (**d**) is 2 cm

presence of an osseous secondary palate). However, many important features indicate that they were more closely related to therocephalians (Hopson and Barghusen 1986) and convergence is the best explanation for features in common with cynodonts (Watson 1921).

The first member of the Bauriidae in South Africa was described in the 1890s, followed by additional discoveries that took place until the middle of the 1970s. Here we present a historical review of the taxonomy of this family.

*Microgomphodon oligocynus* [represented by a small complete skull (Fig. 13.1a; Table 13.1)] and *Microgomphodon eumerus* (represented by a cranial fragment and part of the skeleton) were the first described representatives of what would be called bauriids, although they were originally reported as gomphodont reptiles by Seeley (1895). In a brief account lacking illustrations, Broom (1905) described the skulls of *Sesamodon browni* and *Melinodon simus* (Fig. 13.1b, c; Table 13.1). He allocated these forms to the

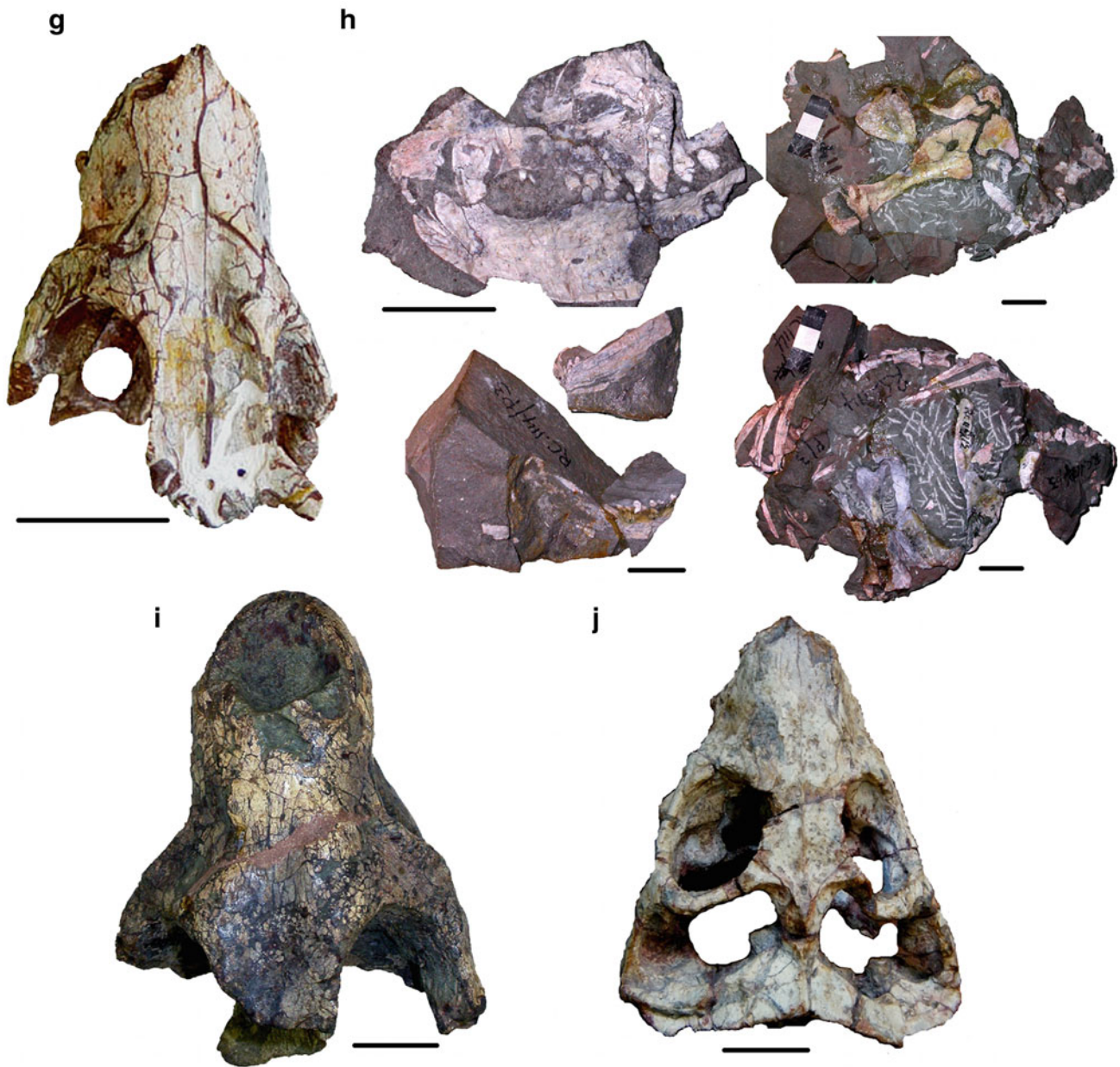


**Fig. 13.1** (continued)

new family Sesamodontidae and placed these new taxa with “*Theriodonts* (or *Cynodonts*)...” but noted that they “may ultimately prove to be the type of a new Suborder connecting *Theriodonts* and Mammals” (Broom 1905, p. 273). Broom (1906) described ‘a new cynodont’ *Aelurosuchus browni* (Fig. 13.1d; Table 13.1) that he thought similar to *Microgomphodon oligocynus*, and later described *Bauria cynops* (Fig. 13.1e; Table 13.1), which he considered a primitive cynodont (Broom 1909). Broom (1911) briefly redescribed *B. cynops*, provided more illustrations, and

proposed it as the type of the new family Bauridae (Broom 1911; the spelling of this family name was later correctly emended to Bauriidae). He recognized *B. cynops* as a cynodont that “retains many of the Therocephalian characters” (Broom 1911, p. 898), and redescribed and illustrated *Sesamodon browni* and *Melinodon simus* (Broom 1911, pp. 913–916). These two species were considered as closely allied and “pretty certainly” belonging to the same family (Broom 1911, p. 916).

**Table 13.1** Nominal species of Bauriidae (see Fig. 13.1)

Taxon	Type specimen
<i>Microgomphodon oligocynus</i> Seeley 1895	NHMUK R3305
<i>Microgomphodon eumerus</i> Seeley 1895	NHMUK R3581
<i>Sesamodon browni</i> Broom 1905	SAM-PK-5865
<i>Melinodon simus</i> Broom 1905	SAM-PK-5866
<i>Aelurosuchus browni</i> Broom 1906	SAM-PK-5875
<i>Bauria cynops</i> Broom 1909	SAM-PK-1333
<i>Baurioides watsoni</i> Broom 1925	NHMUK R4095
<i>Microhelodon eumerus</i> Seeley 1895	NHMUK R3581
<i>Watsoniella breviceps</i> Broili and Schröder 1935	BSP 1934-VIII-13
<i>Sesamodontoides pauli</i> Broom 1950	RC 114
<i>Bauria robusta</i> Brink 1965	BP/1/1685
<i>Herpetogale marsupialis</i> Keyser and Brink 1978–1979	GSN R337

Although Broom (1911) recognized many shared characters between *Sesamodon* and *Bauria*, he did not explicitly include the former taxon in the family Bauriidae. In his phylogenetic tree (Broom 1911, p. 923), *Bauria* appears close to the “Therocephalian Ancestor”, followed by *Aelurosuchus*, whereas the closely related *Melinodon* and *Sesamodon* appear close to the “Mammalian Ancestor”. Watson (1913) considered *Microgomphodon oligocynus* and *Bauria cynops* as members of a common (innominate) family. Watson (1914) described additional specimens of *Bauria* and *Sesamodon* in the Natural History Museum, London. Referring to the latter taxon, Watson (1914, p. 1025; italics ours) states: “This type is probably represented in the British Museum by the anterior part of a skull broken off through the middle of the orbits” (FA was unable to locate this specimen in the Natural History Museum). In addition, Watson (1914, p. 1038) recognized Bauridae (sic), in which he included *Bauria*, *Microgomphodon*, and *Sesamodon*, as a distinct suborder separated from cynodonts.

Among the cynodonts housed in the collection of the American Museum of Natural History, Broom (1915) mentioned and figured a specimen of *Bauria cynops* and another of *Sesamodon browni*. Haughton (1922) described the palate and basicranium of the holotype of *Aelurosuchus browni* and assigned it to the Bauriamorpha. Broom (1925) proposed the new species *Baurioides watsoni* (Fig. 13.1f; Table 13.1) for the skull that was previously described as *Bauria cynops* by Watson (1914), based on differences in postcanine number. Broom (1931) argued that Seeley’s (1895) *Microgomphodon eumerus* comprises a cranial fragment of a bauriid and the skeleton of a cynognathid cynodont and proposed the new combination *Microhelodon eumerus* (Seeley 1895) to name the cranial fragment. Broili and Schröder (1935) described the new species *Watsoniella breviceps* (Fig. 13.1g) based on a partial skull. Successive contributions by Broom (1937) and Boonstra (1938) described the same specimen of *Bauria cynops* housed at

the American Museum of Natural History. Broom (1950) described *Sesamodontoides pauli* (Fig. 13.1h; Table 13.1) based on a fragmentary skull and partial postcranium of which he only illustrated the mandible. Brink and Kitching (1953) described a complete skull and mandible with part of the skeleton of *Bauria cynops* and mentioned an isolated left dentary of a second individual, which was not described. Brink (1963) provided a detailed description of *Bauria cynops*, using the two specimens reported previously by Brink and Kitching (1953) and two new specimens from the collection of the Bernard Price Institute. The last new species to be recognized from the South African Karoo was a partial skull named *Bauria robusta* (Fig. 13.1g; Table 13.1) described by Brink (1965). Finally, Keyser (1973a, b) found a *Sesamodon*-like skull in the Middle Triassic Omingonde Formation of Namibia that was later named *Herpetogale marsupialis* (Keyser and Brink 1977–1978) (Fig. 13.1h; Table 13.1).

The major aim of the present contribution is to provide a detailed description of a new specimen of *Microgomphodon oligocynus*, the best-preserved bauriid specimen yet known, recovered from the *Cynognathus* AZ, Subzone B of the Karoo Basin. We also present a taxonomic review of the southern Africa Bauriidae after firsthand examination of most of the existing specimens. To this end, and as an alternative of linear measurement comparison, we employed Procrustes analysis between the new specimen of *Microgomphodon oligocynus* (SAM-PK-K10160) and the best-preserved specimen of *Bauria cynops* (BP/1/1180). This analysis highlighted several differences between these “morphotypes” that were not perceived by visual inspection. Finally, we present details of the temporal and geographic distribution of these late therocephalian survivors in the Karoo Basin of southern Africa.

Institutional abbreviations: AMNH, American Museum of Natural History, New York City, NY, USA; BP, Bernard Price Institute for Palaeontological Research, University of

the Witwatersrand, Johannesburg, South Africa; BSP, Bayerische Staatssammlung für Paläontologie und historische Geologie, Munich, Germany; GSN, Geological Survey of Namibia, Windhoek, Namibia; NHMUK, The Natural History Museum, London, UK; NMQR, National Museum, Bloemfontein, South Africa; SAM, Iziko, the South African Museum, Cape Town, South Africa; RC, Rubidge Collection, Wellwood, Graaff-Reinet, South Africa. UCMP, University of California Museum of Paleontology, Berkeley, CA, USA; USNM, National Museum of Natural History, Washington, D.C., USA

## Materials and Methods

The new specimen, SAM-PK-K10160, consists of a cranium with mandible in occlusion, four cervical vertebrae (including ribs), and a manus. This specimen was found at the farm Lemoenfontein 44, Rouxville District, South Africa. For this study all holotypes of the nominal southern African bauriid species were examined (see Fig. 13.1; Table 13.1). Non-holotype material examined includes: AMNH 5517, 5622; BP/1/1180, 1679, 1685, 2523, 2837, 3770, 4655, 4678; NMQR 3183 and 3596.

The comparative approach of this work was twofold: (a) detailed inspection of the studied specimens to recognize qualitative variables that can be used for taxonomic purposes; and (b) a Procrustes analysis of two selected specimens representing *Microgomphodon oligocynus* (SAM-PK-K10160) and *Bauria cynops* (BP/1/1180), which are the best-preserved individuals referred to these taxa. The main intention of this approach was to highlight shape differences that may not be recognizable on a discrete character basis to provide further elements for taxonomical distinction. This is part of a study in progress by FA and TJ that will enlarge the sample of specimens studied with this methodology and explore some functional implications related to morphological differences among bauriid skulls.

## Virtual Reconstruction

Computer tomographic scanning was used for virtual preparation of specimens SAM-PK-K10160 and BP/1/1180 in order to digitally separate the cranium and mandible. The specimens were CT-scanned at the Helen Joseph Hospital (Johannesburg, South Africa) on a Philips Brilliance 16 medical CT scanner (under 140 kV, tube current 165 mAs, beam collimation 0.5 cm, interstice distance 0.4 cm). 5.224 pixels per mm and depth 16 bits (unsigned) images were reconstructed using the sharp construction algorithm. The image stack was resampled to 20.898 pixels per mm

and semi-automated routines of segmentation were undertaken using Avizo 6.2.1 software (Visualization Sciences Group, Mérignac, France). Threshold was defined between 2,200 and 4,000 HU, lower and upper level respectively, for automated segmentation routines. Manual segmentation was undertaken in situations where specimen and sediment density, or joint areas between mandible and cranium, were similar. 3D rendered surfaces of the cranium and mandible are shown in Fig. 13.2.

The description of the new material is supplemented with a 3D reconstruction of the specimen (Figs. 13.2, 13.3) which facilitates description of the anterior portion of the palate (concealed by the occluded mandible) (Fig. 13.2b) and reveals details of the postdentary bones in the mandible (Fig. 13.2e, g).

## Correction of Deformation

During fossilization, SAM-PK-K10160 was distorted mostly on its left side (Fig. 13.2). In order to perform Procrustes analysis, correction of the deformation was undertaken by mirroring the less distorted side. Translation and rotation of the less deformed side of the cranium was performed until we achieved anatomical continuation (Zollikofer et al. 1998). Additionally, displacement of the zygomatic arch was corrected using translation and rotation of a portion of the arch until the anterior and posterior ends of this portion achieved anatomical continuation with the suborbital bar anteriorly and the posterior portion of the zygoma, posteriorly. In the mandible, the undistorted right side was mirrored to the left side using the same technique (Fig. 13.3).

## Procrustes Analysis

In order to understand shape correspondence between the two genera of Bauriidae we performed a Procrustes analysis (Gower 1975) using the most complete and best-preserved representative of each taxon. The least squares method was used to find the “best fit” of matrix A (in this case *Microgomphodon oligocynus*—SAM-PK-K10160) to matrix B (*Bauria cynops*—BP/1/1180) under scaling, rotation, and translation (Rohlf and Slice 1990; Dryden and Mardia 1998). Because landmarks provide the foundation of shape in Procrustes analysis, a series of landmarks were defined for the cranium and mandible (Fig. 13.3). Three types of landmarks (anatomical, mathematical, and pseudo-landmarks; Bookstein 1991) were used.

Procrustes analysis was performed using Morphologika (O’Higgins and Jones 2006). The configuration matrix after Procrustes analysis was used to explore the relationships

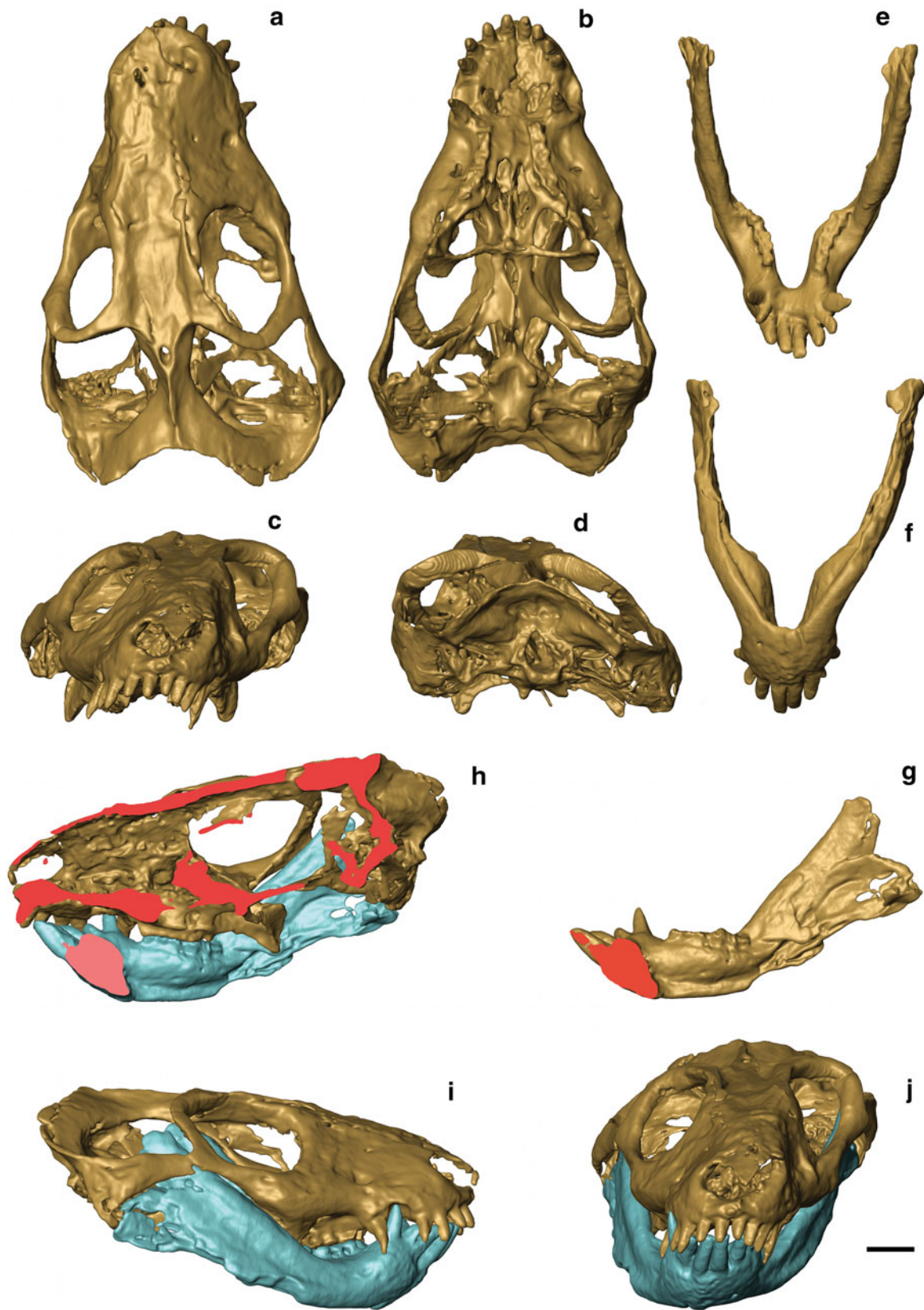


**Fig. 13.2** Virtual reconstruction of *Microgomphodon oligocynus* (SAM-PK-K10160) cranium and mandible from different views. Cranium: **a** dorsal; **b** ventral; **c** anterior; **d** posterior. Mandible: **e** dorsal; **f** ventral; **g** posterior. Cranium and mandible together: **h** medial; **i** lateral; **j** anterior. Scale 1 cm

between these two genera (Fig. 13.4). Landmark surface warp rigid scaled module was used on the Avizo 6.2.1 software to rotate, translate, and scale 3D surfaces and a configuration matrix was produced for each specimen. Surface distance was measured between warped triangulated surfaces. For each vertex of a particular surface, Morphologika computes the closest point on the other surface. The colored map with shading from red to white (Fig. 13.4) represents surface differences between *Microgomphodon oligocynus* and *Bauria cynops*. Dark red indicates greater difference between the two specimens (Fig. 13.4a–d). Results of this analysis were also presented comparing shape configuration matrices for the cranium (Fig. 13.4a', b') and mandible (Fig. 13.4c', d') of *Microgomphodon oligocynus* (SAM-PK-K10160) represented in red and *Bauria cynops* (BP/1/1180) in grey/black.

## Systematic Paleontology

**Therapsida** Broom, 1905

**Therocephalia** Broom, 1903

**Bauriidae** Broom, 1911

*Microgomphodon oligocynus* Seeley, 1895

1905 *Sesamodon browni* Broom: 272

1905 *Melinodon simus* Broom: 273

1935 *Watsoniella breviceps* Broili and Schröder: 23,

Fig. 1

1977–1978 *Herpetogale marsupialis* Keyser and Brink:

91, Fig. 1

1977–1978 *Herpetogale saccatus* Keyser and Brink:

103, Table 5.1 (in error)

**Holotype:** NHMUK R3305, complete skull and lower jaws preserved in occlusion, from an unknown locality in Aliwal North District.

**Referred Specimens:** BSP 1934-VIII-13; SAM-PK-5865, SAM-PK-5866, SAM-PK-K10160; NMQR 3183; NMQR 3596; BP/1/4655; GSN R337.

**Localities:** See Table 13.1.

**Horizon and Age:** Levels of the Burgersdorp Formation corresponding to the faunas of the Subzone A and B of the CAZ, Karoo Basin, South Africa; upper Omingonde Formation, Otjiwarongo Basin, Namibia. Late Olenekian (Subzone A) to Anisian. Specimens collected from Subzone A of the CAZ are the oldest record of the taxon. The material from Namibia was collected high in the upper Omingonde Formation, near the contact with the Etjo Formation (Keyser and Brink 1977–1978) from levels probably of Late Anisian age (Abdala and Smith 2009).

**Diagnosis:** Small member of the Bauriidae presenting a relatively short snout and large orbits of almost equal size as the temporal openings; postorbital bar completed by an

ascending process of the jugal; presence of parietal/pineal foramen; restricted exposure of the frontal on the dorsal orbital margin; presence of suborbital foramen oriented dorsally; short choanae with the vertical keel of the vomer ending near the base of the pterygoid flanges; well-developed, fan-shaped basisphenoidal keel; maxillary shelf curved immediately behind the canine; platform lateral to the post-canine row in the mandible extended anteriorly; vomer participates in the posterior margin of the secondary osseous palate; pterygoid process located anteriorly; presence of a lateral fossa on the posterior portion of the dentary horizontal ramus and on the coronoid process; first lower incisors remarkably large and procumbent; canine placed approximately at mid-length of the snout; postcanine number variable from 5/5 to 7/7; postcanines oval and almost equally wide labially and lingually, and appear broad when observed in labial view.

**Comments:** The diagnostic characters mentioned above separate *Microgomphodon oligocynus* from *Bauria cynops*. These two taxa share a suite of characters indicating a close taxonomic affinity, including presence of a complete osseous secondary palate, dentary processes or shelves lateral to the postcanine series (clearly better developed in *M. oligocynus*), and expanded postcanine crowns which manifest occlusion.

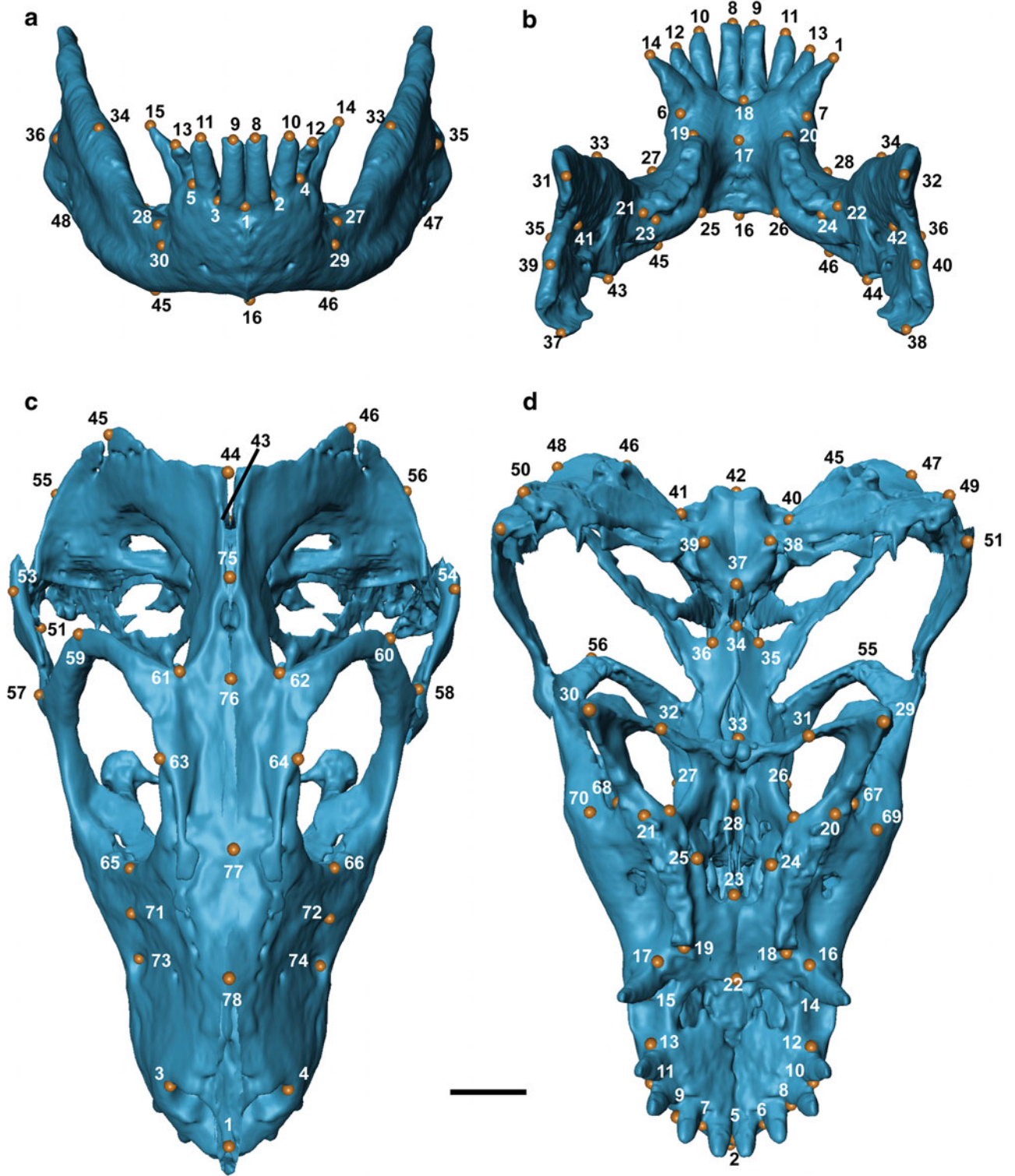
## Description

### General Preservation

The preservation of SAM-PK-K10160 is excellent, with almost all sutures of the skull clearly visible (Fig. 13.5). The mandible is preserved in occlusion and the crowns of the postcanines are visible labially and lingually. Postdentary bones of the mandibles are preserved with the dorsal portion of the reflected lamina of the angular present on both sides, the ventral parts of the laminae being missing. The right lateral wall of the braincase and interorbital regions are completely preserved. The palate is preserved with all bones in their natural position, and in the basicranium the central para-basisphenoid keel and both stapes are well-preserved. Four cervical vertebrae, including the atlas-axis complex, first complete, and the second and third partial cervical ribs are preserved in situ.

### Size and General Proportions

The basal skull length of SAM-PK-K10160 is 87.4 mm, similar to that of GSN R337 which is 88.57 mm. These two specimens are the largest representatives of the species. The



◀ **Fig. 13.3** Location of cranio-mandibular landmarks defined for the Procrustes analysis. **Mandibular landmarks:** (1) Anterior symphysis, below the two anterior incisors of both sides. (2;3) Between the base of first and second incisors; (4;5) between the base of second and third incisors; (6;7) behind the canine; (8;9) tip of the first incisor; (10;11) tip of the second incisor; (12;13) tip of the third incisor; (14;15) tip of the canine; (16) ventral symphysis. (17) symphysis where the dentaries contact each other posteriorly. (18) Symphysis behind the first incisors of both sides. (19;20) Anterior margin of the postcanine series (towards the center of the tooth); (21;22) posterior margin of the postcanine series (towards the center of the tooth); (23;24) medial corner of the last postcanine; (25;26) maximum internal curvature point of the dentary (observed in ventral view); (27;28) anterior base of the coronoid process; (29;30). Anterior margin of the lateral canal of the dentary; (31;32) tip of the coronoid process; (33;34) half distance between landmark 27 and 31; (35;36) junction between the dentary and surangular in lateral view; (37;38) cranio-mandibular joint; (39;40) half distance between landmark 35 and 37; (41;42) end of the dorsal margin of the meckelian canal (represented as a bulged expansion of the dentary below the teeth); (43;44) angular process (where finish the embracing Meckelian canal of the dentary); (45;46) half distance between landmark 16 and 43; (47;48) contact between dentary and angular in lateral view. **Cranial landmarks:** (1) Tip of the snout; (2) distal middle point of the snout. (3;4) dorsoposterior margin of nasal opening; (5) between first incisors of each side; (6;7) between base of incisors 1st and 2nd; (8;9) between base of incisors 2nd and 3rd; (10;11) between base of incisor 3rd and 4th; (12;13) posterior

margin of incisors; (14;15) anterior margin of canine; (16;17) posterior margin of canine; (18;19) anterior margin of postcanine row; (20;21) posterior extension of postcanine row; (22) central portion of the osseous palate at the level of the canine; (23) posterior end of the palate; (24;25) most internal point of maxillary curvature; (26;27) anterior portion of suborbital vacuity; (28) posterior margin of the vomer; (29;30) tip of pterygoid flange; (31;32) posterior portion of suborbital vacuity; (33) anterior margin of interpterygoid vacuity; (34) posterior margin of the interpterygoid vacuity; (35;36) opening of the quadrate ramus of pterygoid in the basicranial grider; (37) basal tubera anterior margin of basisphenoid; (38;39) basal tubera; (40;41) opening of the jugular foramina; (42) occipital condyle; (43) dorsal central point of foramen magnum; (44) end of the sagittal crest; (45;46) point between landmarks 45 and 53, 46 and 54 respectively; (47;48) contact of the posterior corner of temporal fossa; (49;50) squamosal lateral surface that contact quadrate; (51;52) squamoso-jugale suture in the ventral margin of the zygoma; (53;54) zygoma dorsal margin; (55;56) point between landmarks 45 and 44, 46 and 44 respectively; (57;58) posteroinferior margin of the orbit; (59;60) tip of postorbital process; (61;62) union postorbital bar and skull; (63;64) centre of dorsal margin of orbit; (65;66) front of the orbit; (67;68) base of pterygoid process; (69;70) start of ventral margin of zygoma; (71;72) anterior border of lacrimal bone; (73;74) infraorbital foramen on the snout; (75) point between landmarks 44 and 76; (76) anterior margin of temporal region (no repetitive); (77) translation of the anterior portion of the orbit in dorsal view of the skull; (78) point between landmarks 1 and 77

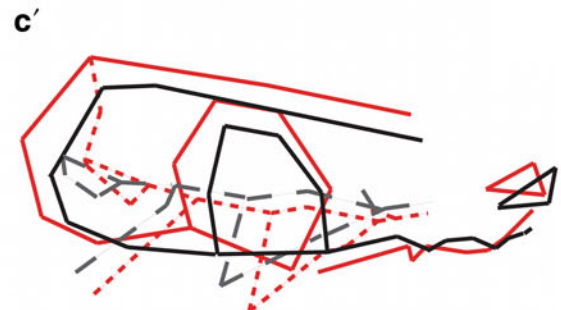
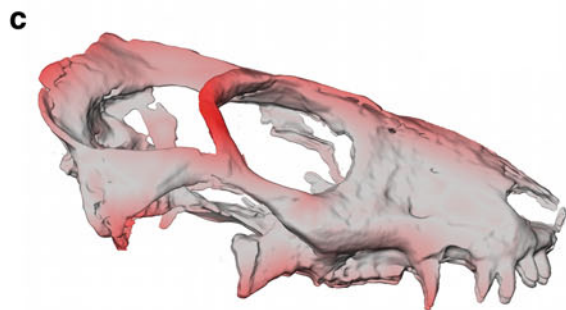
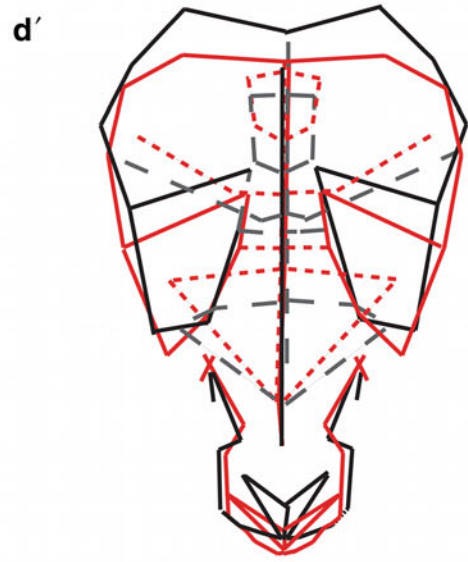
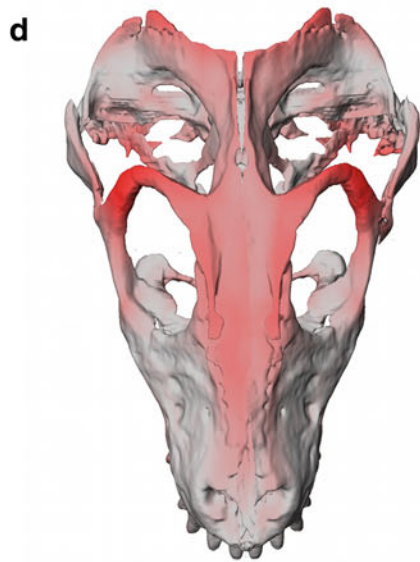
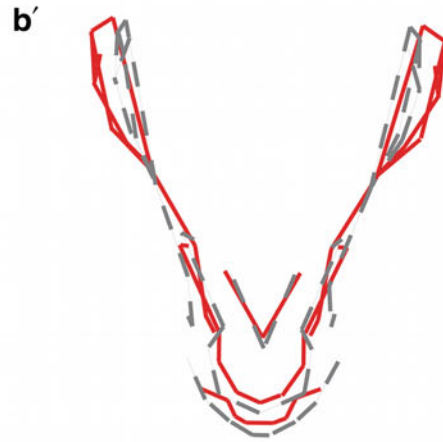
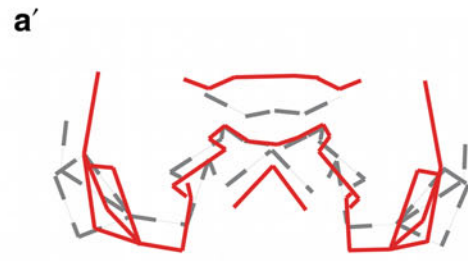
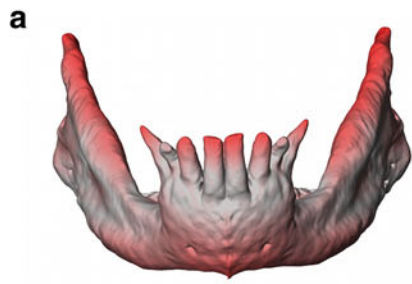
skull has a triangular outline in dorsal view, with the maximum width of the skull (61.0 mm) at the posterior portion of the temporal region (Figs. 13.2a–d, 13.3a, 13.4a). Although the snout is short compared to other therocephalians, it is the longest region of the skull, representing 45 % of the basal skull length (Fig. 13.6). The orbital and temporal regions are subequal, respectively representing 30 and 29 % of the BSL. In GSN R237 the cranium proportions are slightly different, particularly in the snout (Fig. 13.6) (Table 13.2).

### Snout and Orbits

The premaxilla forms the anterior margin of the snout and has a well-developed, dorsally directed ascending process. As the anterior portions of both nasals are preserved as an internal cast it is possible to observe the protrusion of the dorsal portion of the premaxillary ascending process between the nasals (Fig. 13.5a; contra Keyser and Brink 1977–1978). The anterior premaxillary foramen is located at the base of the ascending process near the suture with the other premaxilla. An elliptical external naris is directed anterolaterally, with its antero-posterior axis being longer than the dorsomedial axis (Figs. 13.2c, i, 13.5a, b). The anterior facial exposure of the premaxilla is restricted as it is covered by part of the facial extension and the intranarial process of the septomaxilla (Fig. 13.5b). The lateral

exposure of the premaxilla is highest at its posterior end where the facial process of the septomaxilla is directed dorsoposteriorly (Fig. 13.5b) and the posterior margin of the premaxilla is slightly behind the level of the posterior margin of the external naris. The facial process of the septomaxilla is interposed for a long distance between the maxilla and the nasal, with a septomaxillary foramen placed at the base of the process and limited by the maxilla posteriorly (Fig. 13.5b). The intranarial process of the septomaxilla is reduced, in comparison with that of the scylacosaurid *Glanosuchus* (van den Heever 1994: Figs. 1, 2), and they do not contact the process of the opposite side. The dorsal projection of the intranarial process is small (Fig. 13.2i).

The maxilla forms a shelf lateral to the postcanine teeth that extends from immediately behind the canine to below the anterior margin of the orbit (Figs. 13.2b, i, 13.5b). In lateral view the maxillary shelf is somewhat concave behind the canine and slightly convex below the orbits. A series of anteriorly oriented nutritive foramina are present at the base of the canines and anterior to this tooth (Fig. 13.5b). A small dorsally oriented infraorbital foramen is present at the level of the canine buttress, and a small nutritive foramen is positioned immediately ventral to the “infraorbital foramen” on both sides of the snout (Figs. 13.2a, i, 13.5a, b). The posterior extension of the maxilla extends below the jugal reaching the middle of the orbit (Fig. 13.5b). The surface texture of the maxilla on the posterior extension is different from the rest of the bone,



◀ **Fig. 13.4** Surface distance colour map expressed in whitish and reddish indicating lower and higher differences respectively, between the cranium (a, b) and mandible (c, d) of *Microgomphodon oligocynus* (SAM-PK-K10160) and *Bauria cynops* (BP/1/1180). Shape configuration matrix for the cranium (a', b') and mandible (c', d') of

*Microgomphodon oligocynus* (SAM-PK-K10160) in red and *Bauria cynops* (BP/1/1180) in grey/black. In a' and b', solid lines represents dorsal view of cranium and dots/dash lines the ventral view of cranium. In c' and d', solid red lines represents *M. oligocynus*, whereas the dashed grey lines corresponds to *B. cynops*

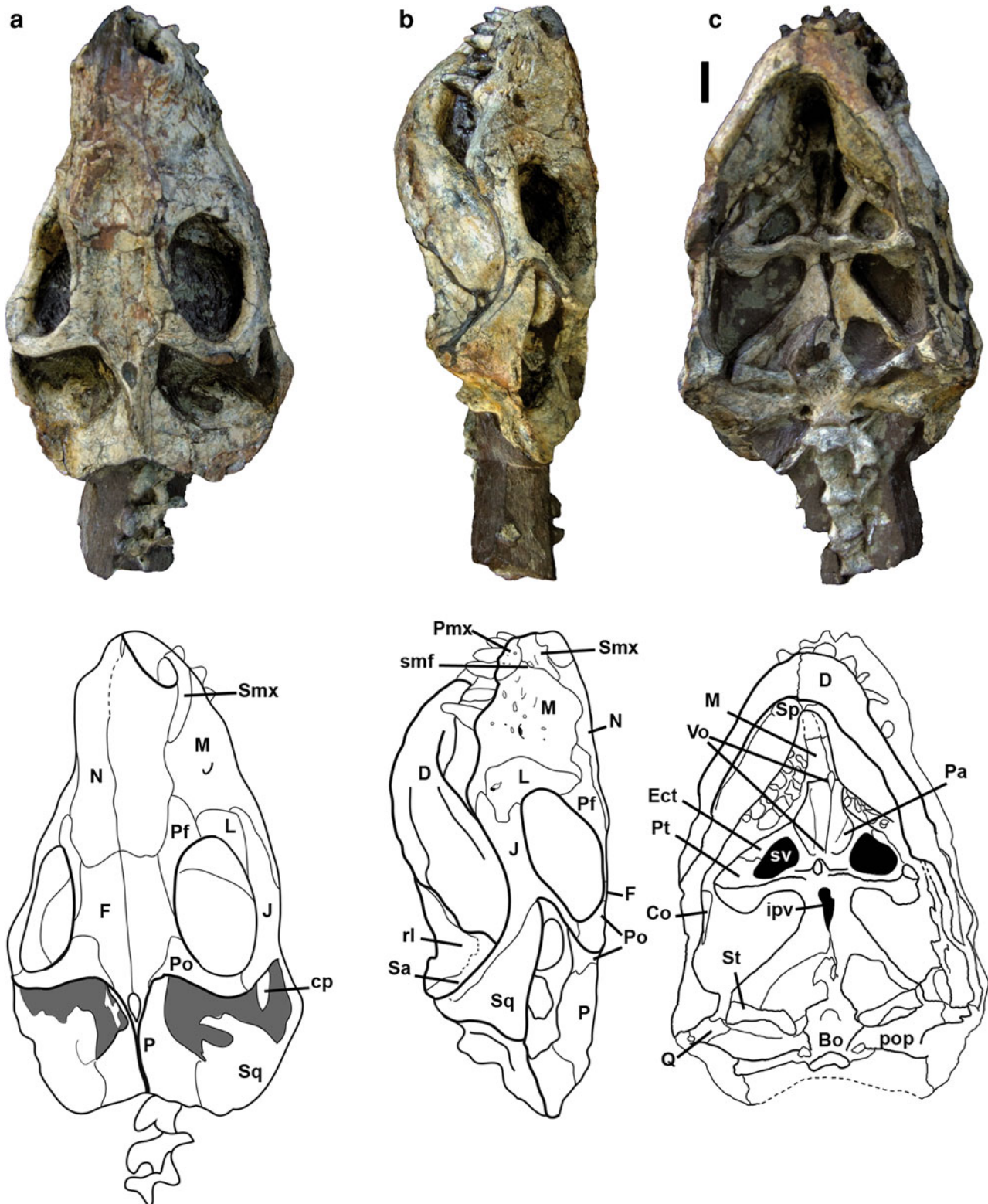


**Fig. 13.5** SAM-PK-K10160. Photo and drawing in a dorsal, b lateral and c ventral views. Bo Basioccipital, Co coronoid, cp coronoid process, d dentary; Ect ectopterygoid, f frontal, ipv interpterygoid vacuity, J jugal, L lacrimal, M maxilla, N nasal,

P parietal, Pf prefrontal, Po postorbital, pop paraoccipital process, Pt pterygoid, Q quadrate, rl reflected lamina, Sa surangular, smf septomaxillary foramen, Smx septomaxilla, Sp splenial, Sq squamosal, St stapes, sv suborbital vacuity, Vo vomer. Scale 1 cm

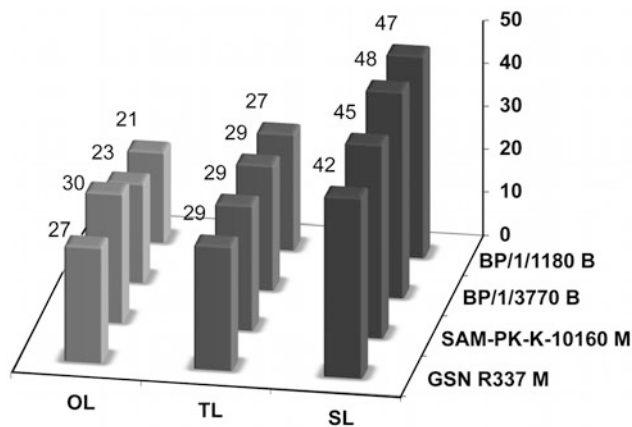


**Fig. 13.6** Cranial proportions of selected specimens of Bauriidae: Proportion of the orbital length (OL), snout length (SL) and temporal length (TL) in relation to the basal cranial length. *B* are specimens of *Bauria cynops* and *M* of *Microgomphodon oligocynus*

**Table 13.2** Measurements of SAM-PK-K10160 (in mm, except for postcanine number)

Basal cranial length	87.36
Dorsal cranial length	89.43
Snout length	39.22
Orbital length	26.53
Temporal length	25.18
Snout width at canine level	28.6
Maximum width of cranium	62.68
Interorbital width	19.19
Orbit diameter	25.17
Occiput width	35.44
Occiput height	24.27
Posterior root of the zygoma height	16.32
Palate length	34.65
Suborbital vacuity length	5.67
Length from tip of snout to pterygoid wings in the middle of the cranium	54.13
Basicranial girder width anteriorly	8.97
Basicranial length	14.07
Mandible length	74.24
Dentary length on the inferior margin	51.59
Zygoma length from orbit to posterior margin	42.54
Epipterygoid height	17.2
Epipterygoid width at the dorsal margin	9.16
Incisor–canine extension (until posterior margin of the canine)	28.36
Postcanine number	6/6

having faint striations directed posteriorly, probably related to adductor muscle attachment. The broadest portion of the wide nasal contacts the anterior margin of the prefrontal (Figs. 13.2a, 13.5a). The suture between the nasal and

frontal forms an obtuse angle (approximately 150°; Figs. 13.2a, 13.5a).

The anterior margin of the lacrimal forms a convex suture with the maxilla which continues ventrally to the jugal-maxilla suture (Fig. 13.5a, b). Dorsoventrally, the lacrimal extends from the middle of the orbit to its base. The lacrimal foramen has a variable placement on the bone, being on the facial surface on the right side and on the orbital surface on the left.

The prefrontal is triangular on the facial region, with the anterior tip of the bone interposed between nasal and maxilla (Fig. 13.5a). A narrow posterior projection of the prefrontal extends half way along the dorsal rim of the orbit, thus restricting participation of the frontal in the dorsal margin of the orbit (Fig. 13.5a).

In dorsal view the frontal is broad but tapers posteriorly from its contact with the postorbital (Fig. 13.5a). The frontal has a small exposure on the dorsal orbital rim behind the prefrontal and ends at the level of the postorbital bar, in front of the pineal foramen. The frontals and the posterior portion of the nasals form a depressed area between the orbits (Fig. 13.2a, c).

The sutural contact between the postorbitals and the frontals is oriented anterolaterally and extends posteriorly slightly beyond the pineal foramen (Fig. 13.5a). Posteriorly, the parietals form a short sagittal crest (Figs. 13.2a, 13.5a).

## Palate

There is a well-developed palatal foramen located medial to the paracanine fossa and limited by the premaxilla anteriorly and by the maxilla in the remaining margin. The paracanine fossa is a well-developed concavity located anterior to the upper canine (Figs. 13.2b, 13.5b). The osseous secondary palate is formed by a large extension of the maxilla and a small contribution of the vomer, posteriorly and in the middle of palate (Figs. 13.2b, 13.5c, 13.7a). The maxilla forms a long posterior and lateral projection which extends beyond the postcanine series, whereas the vomer forms a posteriorly directed keel that bisects the choanae (Figs. 13.5c, 13.7a). The area from the choanae to the pterygoid processes is remarkably short in comparison with that of *Bauria*, because of a notable reduction of the sub-orbital fossa. The palatines form the lateral walls of the choanae and the suture between palatine and pterygoid is not visible. A well-developed ventromedian crest is present at the base of the transverse process of the pterygoid in front of the interpterygoid vacuity (Figs. 13.2b, 13.5c, 13.7a). The circular suborbital fossa is small and the postero-lateral margin of the transverse process has a rounded projection directed posteriorly (Figs. 13.5c, 13.7a), which is of variable

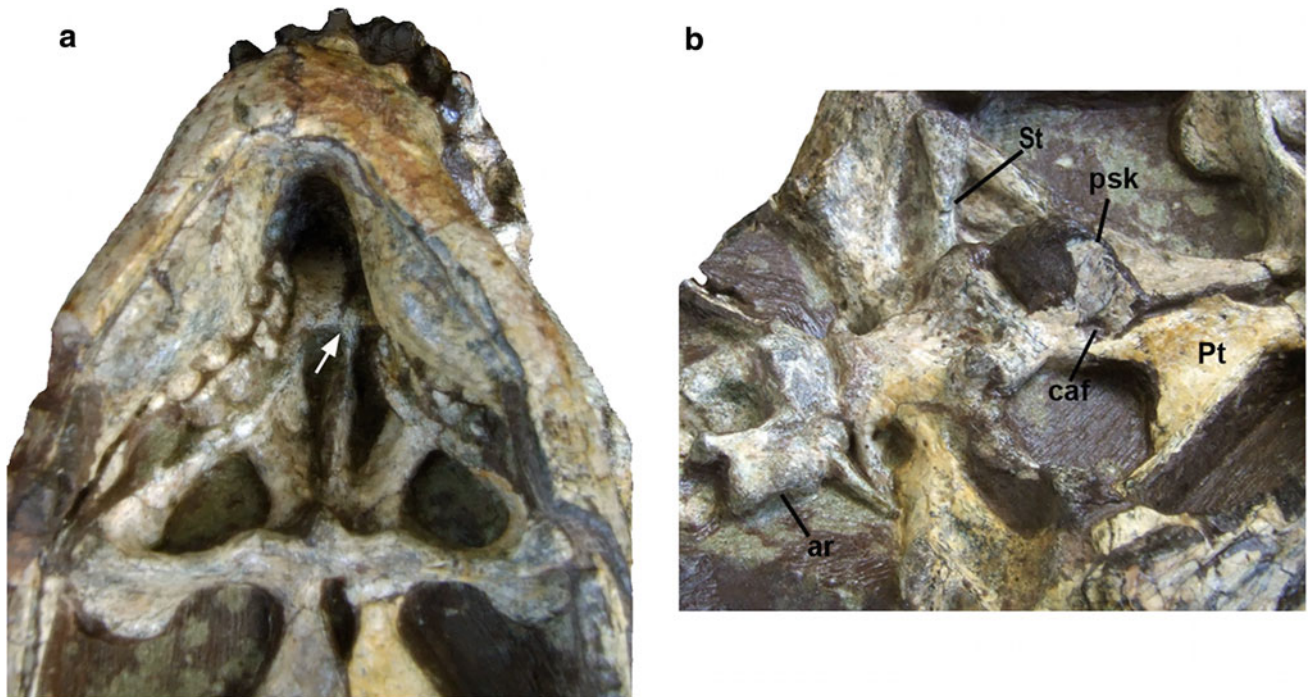


**Fig. 13.7** SAM-PK-K10160. **a** Detail of the palate. *Arrow* indicates vomer contribution in the formation of the osseous palate. **b** Detail of the basicranium. Anterior to the right. *ar* atlantal rib, *caf* carotid foramen, *psk* parasphenoidal keel, *Pt* pterygoid, *St* stapes

proportions in the different specimens (that of GSN R337 is much less developed).

### Zygoma and Temporal Region

The temporal opening is approximately rectangular, wider transversely. The zygomatic arch, including the suborbital and temporal bars, is formed by the posterior portion of the maxilla, the jugal, and the squamosal (Fig. 13.5b). The suborbital bar is slightly longer than the temporal bar and the ventral edge of the arch is convex anteriorly and concave in its central and posterior portions (Fig. 13.5b). At the anterior part of the orbit, the arch (comprising maxilla and jugal) is very high and robust. Posteriorly, the arch decreases to only half of its height at the level of the middle of the orbit and comprises only jugal (Fig. 13.5b). The posterior projection of the jugal extends almost as far as the end of the zygomatic arch. Posteriorly, the zygomatic arch becomes higher and is formed by the squamosal (Fig. 13.5b). The postorbital projection of the jugal is directed dorsally and contacts the postorbital halfway up the orbit (Fig. 13.5a, b).

The squamosal, which forms the posterior portion of the zygomatic arch, expands posterodorsally to form part of the occipital crest (Fig. 13.5b). This overhangs the ventrally directed squamosal sulcus in the area where the squamosal

contacts the tabular and paroccipital process. In posterior view the squamosal forms a shallow 'V'-shaped groove contacting the quadrate laterally and the paroccipital process medially.

The quadrate is only visible posteriorly as a rectangular bone having a wide horizontal (and presumably also anterior) contact with the articular (Fig. 13.2b).

### Braincase and Basicranial Girder

The basicranial girder is wide anteriorly, where it is positioned between the quadrate rami of the pterygoids, and narrows posteriorly (Figs. 13.2b, 13.5c). A triangular interpterygoid vacuity is present at the anterior margin of the girder, behind the base of the central roots of the pterygoid lateral processes. The basioccipital-basisphenoid plate is pentagonal and no sutures are recognizable between these bones (Figs. 13.5c, 13.7b). A large, semilunar occipital condyle is located posteriorly and a well-developed, ventrally oriented jugular foramen is present anterolateral to the condyle. The robust basisphenoidal tubera are positioned on the anterior portion of the basisphenoid (Figs. 13.5c, 13.7b) and have a deep concave area between them. A remarkably high, fan-shaped parasphenoidal rostrum (Figs. 13.2b, 13.7b) is present anterior to the tubera, and the right carotid foramen is preserved at the base of the

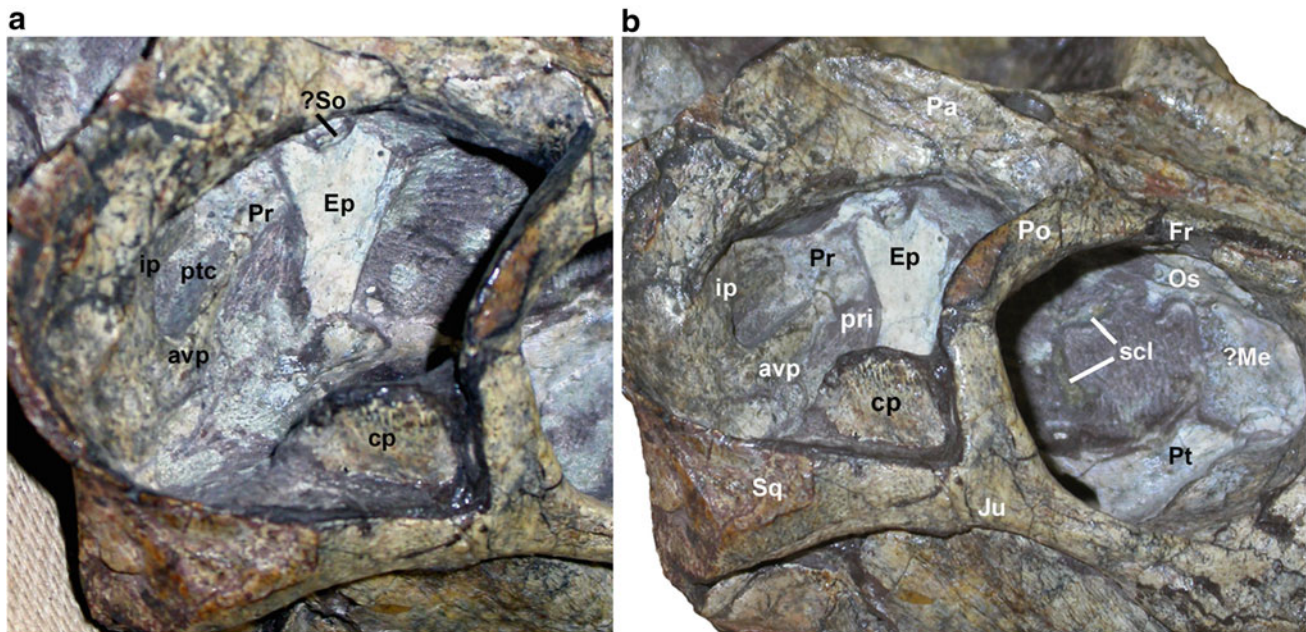


**Fig. 13.8** SAM-PK-K10160. Detail of the **a** lateral wall of the skull; **b** interorbital region. *avp* antero-ventral process of the squamosal, *cp* coronoid process, *Ep* epipterygoid, *Fr* frontal, *ip* intermediate process of the squamosal, *Ju* jugal, *M* mesethmoid, *Os* orbitosphenoid,

*Pa* parietal, *Po* postorbital, *Pr* prootic, *pri* prootic incisure, *ptc* posttemporal canal, *Pt* pterygoid, *scl* sclerotic bones, *So* supraoccipital, *Sq* squamosal

rostrum. The paroccipital process of the opisthotic is narrow proximally and remarkably expanded distally, with the quadrate and occipital portion well-separated by a slight concavity (Fig. 13.7b).

The stapes, preserved in situ on both sides of the skull, is a cylindrical bone with both extremities expanded equally, and lacking a stapedia foramen (Fig. 13.7b). Its distal end is in contact with the paroccipital process dorsally and, visible only on the left side, with the quadrate distally.

### Lateral and Interorbital Walls

In lateral view, the epipterygoid has a thin base and progressively increases in anteroposterior length toward its dorsal margin (Fig. 13.8a). On the left side, a short, anterior projection is present at its base. On the right side of the cranium, the posterodorsal portion of the epipterygoid seems to be superposed by the supraoccipital (Fig. 13.8a). The prootic is visible with its anterior margin in contact with the epipterygoid behind the dorsal third of the lamina and has short, paired posterolateral projections which contact a long projection of the squamosal laterally. The latter bone has two large and important processes: the intermediate process, in contact with the posterodorsal process of the prootic; and the anteroventral process, in contact with the central process of the prootic (Fig. 13.8a). An elliptical,

well-developed post-temporal foramen is limited by these processes. The prootic incisure is located behind the epipterygoid, ventral to the body of the prootic and anterior to the connection between the anteroventral process of the squamosal and the central process of the prootic.

An ovoid interorbital vacuity is located in front of the anterior margin of the lamina of the epipterygoid and extends anteriorly to the ossified interorbital septum (Fig. 13.8b). Small and fragile bones in the right interorbital vacuity are interpreted as sclerotic ossicles. A thin orbitosphenoid is located dorsally and extends the length of the orbit. The left and right orbitosphenoids together form a 'V'-shaped structure, which is continued ventrally by an interorbital septum located in the anterior third of the orbit. Ventrally, this septum contacts the palatine and pterygoid.

### Occiput

Most of the occipital region is masked by the cervical vertebrae (Fig. 13.5). Description of this region is based on digital preparation of the specimen (Fig. 13.2d). The occiput is triangular, with the foramen magnum having half of the height of the occipital plate (Fig. 13.2d). The dorsally situated interparietal bears a well-developed median ridge that continues ventrally onto the supraoccipital. The large tabular occupies a quarter of the occipital plate and meets

the interparietal, supraoccipital, and exoccipital medially by means of a suture which extends obliquely in a ventrolateral direction. The tabular does not form part of the margin of the post-temporal fenestra. The ventral portion of the occiput comprises the paroccipital process which forms the base of the post-temporal fenestra and has a ventromedial projection on the occipital ventral margin. The lateral margin of this process forms a faint ridge that continues dorsally as a well-defined ridge on the suture between the lateral margin of the tabular and the squamosal.

## **Mandible**

The dentary has a boomerang-shaped outline. The ventral margin of the bone is convex (Figs. 13.2i, g, 13.5b). The anterior portion of the dentary is high and has a very strong symphysis that maintains the anterior mandibular rami in its natural placement (Fig. 13.5c). A poorly defined dentary angle is present below the level of the middle of the orbit. The coronoid process is oriented obliquely and extends dorsally behind the postorbital bar (Figs. 13.2i, 13.5b), so that the process is located in the anterior portion of the temporal opening and near to the zygomatic arch. A fossa, delimited by the posteroventral margin of the dentary and the dorsal margin of the coronoid process, extends anteriorly on the coronoid and part of the horizontal processes of the dentary (Fig. 13.5b).

Behind the dentary symphysis a laminar splenial is present and meets its counterpart (Fig. 13.5c) in the midline. In SAM-PK-K10160, only the anterior part of the splenial is preserved and extends posteriorly as far as the level of the diastema between the lower canine and first postcanine. Further posteriorly, just below the internal expansion at the implantation of the postcanines, there is evidence of the original extent of the splenial: a shallow, horizontal canal close to the ventral margin of the dentary (Figs. 13.2g, h, 13.5c). The angular and prearticular form a stout bar, which is covered medially by a large coronoid bone, which was only possible to observe in CT images. This bone is preserved in contact with the pterygoid process of the cranium. Only the dorsal-most portion of the reflected lamina is preserved on both sides of the mandible (Fig. 13.5b). It is a thin plate which has a small, rounded area overhanging the remaining lamina on the right side. The medial portion of the bar formed by the prearticular is lateromedially expanded in the region of the craniomandibular articulation (Fig. 13.2f). No suture is visible between this element and the articular. The surangular is a strip of bone more developed in height posteriorly. On the medial side of the mandible the surangular forms a semi-circle and reaches its greatest height at a level just below the

top of the coronoid process (Fig. 13.2g). In lateral view, the surangular forms an overhanging strip of bone dorsal and posterior to the margin of the reflected lamina.

## **Dentition**

The dental formula of the specimen is I4/3-C1/1-PC6/6. Only the most distal parts of the incisors have enamel as evidenced by their light brown colour, whereas the white basal portions of the exposed ‘crowns’ probably comprise only dentine. The upper incisors are smoothly conical, directed ventrally (Fig. 13.2c, i), and progressively increase in size posteriorly. The lower incisors are large and procumbent, with the first one being remarkably large, more than the double of the size of the upper incisors (Fig. 13.2e, i, j). Lower incisors reduce in size posteriorly; the second lower incisor is smaller than the first, but larger than the upper incisors (Fig. 13.2c). The third lower incisor is smaller than the upper incisors (Fig. 13.2e, j). The upper canine is located half way along the length of the snout behind a well-defined paracanine fossa that accommodates the lower canine in occlusion (Fig. 13.2a, i). The upper canine is almost twice the size of the first upper incisor, but smaller than the first lower incisor (Fig. 13.2i). Serrations are absent on the canine and all incisors.

All postcanines are of similar size with the exception of the smaller last lower postcanine (Fig. 13.5c). As the teeth are tightly occluded, postcanine crown morphology is only partially visible and only their convex labial and lingual sides are evident. On the left side (the less distorted in relation to the mandible, but more distorted relative to the cranium) each upper postcanine occludes with two teeth of the mandible. On the right, each upper postcanine occludes with only one postcanine (Fig. 13.5c).

## **Cervical Vertebrae**

Four cervical vertebrae are preserved in articulation with the cranium (Fig. 13.9a–c). The axial centrum is larger than subsequent ones and all of them show a marked ventral midline keel (Fig. 13.9b). The atlas neural arch has a short dorsal plate with a small posterior projection representing the postzygapophysis and an additional ventral projection. The atlantal intercentrum is a large rectangular plate. Both the lateral projection of the intercentrum and the ventral projection of the neural arch are in contact with the atlantal rib (Figs. 13.7b, 13.9b) which is a large quadrangular plate with a short distal fusiform projection. From the right side

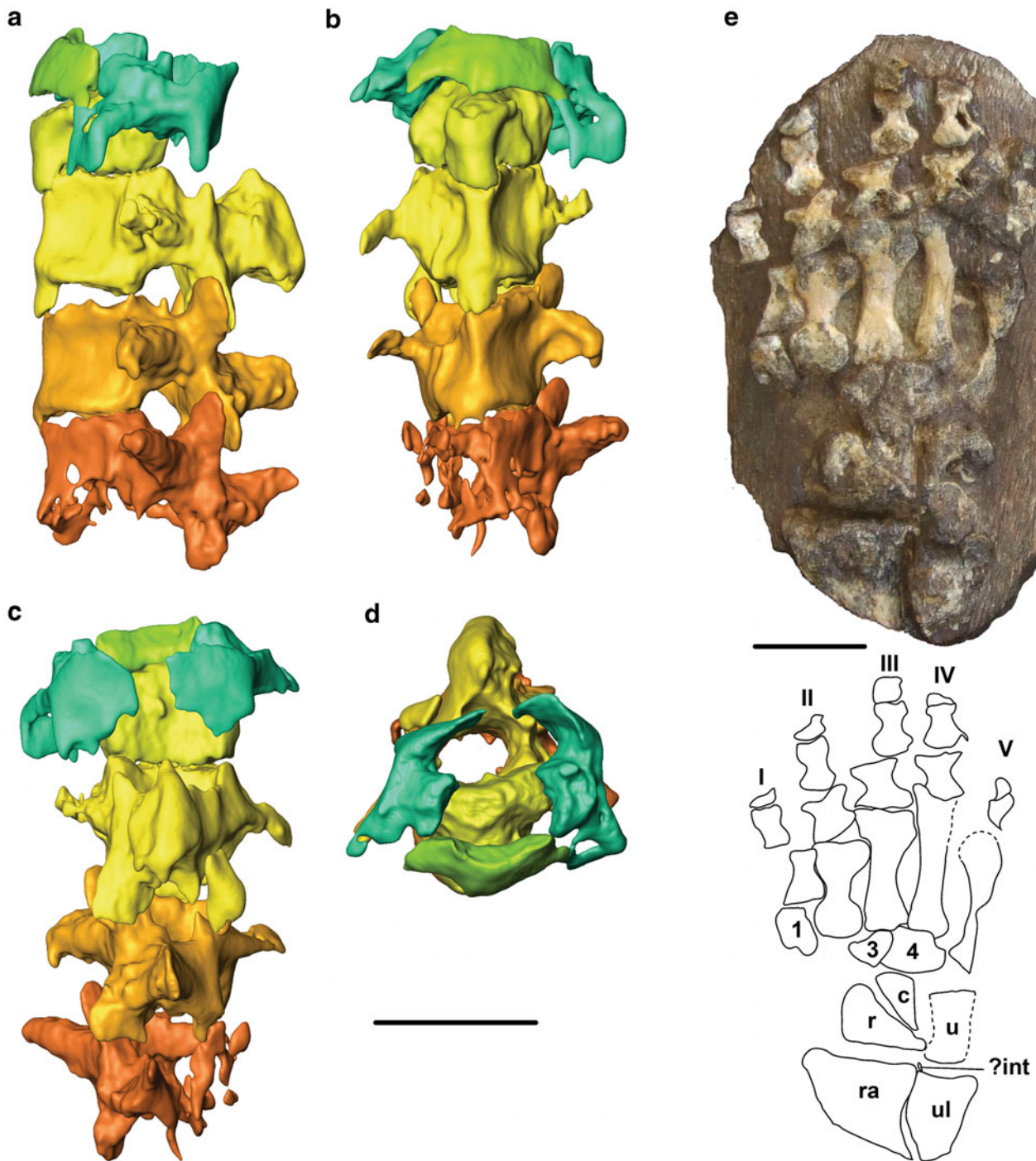


**Fig. 13.9** SAM-PK-K10160. Virtual reconstruction of cervical vertebrae; **a** lateral, **b** ventral, **c** dorsal; and **d** anterior views; **e** right manus in dorsal view. *c* lateral centrale, *int* intermedium, *r* radiale, *ra* distal end of the radius, *u* ulnare, *ul* distal end of the ulna, *1-4* indicate

distal carpals; *I-V* indicate digits. *Dashed lines* indicate lack of bone in the metacarpals and margin of the bone observed in ventral view in the case of the ulnare. Scale 1 cm

there is a contact between the atlas arch and the axis through the atlantal postzygapophysis (Fig. 13.9a).

The neural spine of the axis, which is expanded distally and forms a bulbous structure at its distal end, is only

slightly larger than those of the remaining cervical vertebrae (Fig. 13.9c). The postzygapophyses of the axis are well-developed and articulate horizontally with the prezygapophyses of the third cervical. An axial transverse process is

located at the level of the base of the prezygapophysis and articulates with the proximal portion of the rib. Neural arches of the two remaining cervicals (C3 and C4?) are the same height as the axis, but they are progressively shorter posteriorly (Fig. 13.9a). As in the axis, articular facets between zygapophyses are horizontal in these vertebrae.

## Manus

The distal portions of radius and ulna are poorly preserved, with the radial larger than the ulnar portion. Seven carpal bones are visible in dorsal view (Fig. 13.9e). The triangular radiale shows a convex medial margin and a slight depression toward its medial side. This bone is more exposed dorsally than ventrally. The presence of the intermedium is inferred from a small osseous surface preserved close to the distal margins of the ulna and radius. The lateral centrale is also triangular and its pointed end is positioned between the radiale and the ulnare. The ulnare does not have a clear morphology in dorsal view, but ventrally is a quadrangular bone. Three distal carpals are preserved (Fig. 13.9e). The larger, interpreted as the third carpal is in contact with the ulnare, intermedium, and second distal. In ventral view the third carpal shows a rectangular morphology (wider than long) and a visible depression occupying two-thirds of the ventral surface of the bone. The smaller, triangular second carpal contacts parts of the third and second metacarpals. First distal carpal is larger than the second and smaller than the third. The first distal carpal is roughly quadrangular and has a low medial portion separated from the higher lateral portion by a well-marked concavity. Along its distal margin, it is in contact with the entire proximal surface of the first metacarpal; laterally, it meets the medial portion of the proximal surface of the second metacarpal (Fig. 13.9e). In addition, two *ex situ* bones located below the fifth, fourth and third metacarpals are probably remains of the other carpals.

The fourth and fifth metacarpals are long and the fourth is more robust than the fifth. Metacarpals three to one are successively shorter. The entire lateral margin of the first metacarpal is in contact with the central to distal portion of the lateral margin of the second metacarpal (Fig. 13.9e). The proximal portions of the second and third metacarpals are in contact, and the distal projection of the second metacarpal meets part of the diaphysis of the third metacarpal. This pattern of contact is also present between the third and fourth metacarpals. The second metacarpal is expanded at both the proximal and distal ends with the

distal end being the largest. In contrast, the first metacarpal is much more expanded on the proximal end (Fig. 13.9e). The preserved phalanges are 2, 3, 3, 2(?), 2(?) (Fig. 13.9e). All are robust and quadrangular, with the proximal end usually more transversely expanded than the distal. No ungual phalanges are completely preserved (Fig. 13.9e).

## Comparison of Bauriid Species by Procrustes Analysis

The cranium of *Microgomphodon oligocynus* (based on SAM-PK-K10160) differs from that of *Bauria cynops* (based on BP/1/1180) in the following features: (1) cranium is higher and slightly larger, but less wide (Fig. 13.4a, a', b, b'); (2) snout is higher (Fig. 13.4b'); (3) nasal opening ovoid compared to the elliptical and more anteriorly oriented opening of *B. cynops* (Fig. 13.4b, b', a'); (4) orbit rounded, relatively larger, and more anteriorly oriented (Fig. 13.4b', a'); (5) posterior angle of the zygoma much more pronounced (Fig. 13.4b, b'); (6) projection of the pterygoid process placed further anteriorly (half way along the cranial length) (Fig. 13.4b, b'); (7) lateral margin of the pterygoid process more robust and lateral margin of the suborbital vacuity directed inward (these two trends probably play an important role in the reduction of the size of the suborbital vacuity in *M. oligocynus*); (8) internal choanae less expanded antero-posteriorly (Fig. 13.4a'); (9) anterior and posterior margins of the postcanine series more expanded and more outwardly directed (Fig. 13.4a, a'); (10) canines more posteriorly curved (Fig. 13.4b); (11) incisors located more inwardly (Fig. 13.4b').

In the mandible, the major differences between *Microgomphodon oligocynus* (SAM-PK-K10160) and *Bauria cynops* (BP/1/1180) are: (1) higher symphysis, less elongated in cranial view (Fig. 13.4c, c'); (2) horizontal ramus much more elevated and the corpus of the mandible relatively short (Fig. 13.4c', d'); (3) higher and more laterally directed coronoid process (Fig. 13.4c, c', d, d'); (4) depression of the posterior portion of the dentary deeper (Fig. 13.4c); (5) angular bone posterior to the dentary located more ventrally (Fig. 13.4c'); (6) shelf lateral to postcanines more concave (Fig. 13.4d); (7) postcanine series more curved laterally (Fig. 13.4d, d'); (8) incisors and canines relatively higher and more developed (Fig. 13.4c, d); (10) canines directed dorsally, whereas they are anteriorly oriented in *B. cynops* (Fig. 13.4d); (11) presence of diastema between the first postcanine and the canine (Fig. 13.4d, d').

**Table 13.3** Cranial length and selected characters of specimens studied

Taxa	Cranial length (mm)	Postcanine number	Postorbital bar	Pineal foramen
<i>Microgomphodon oligocynus</i>	65	6	Complete	Present
<i>Sesamodon browni</i>	*80	6	Complete	?
<i>Melinodon simus</i>	?	At least 7	?	?
<i>Watsoniella breviceps</i>	*85	6	?	?
<i>Herpetogale marsupialis</i>	89	5	Complete	Present
<i>Bauria cynops</i> (holotype)	*122	10/11	Incomplete	Absent
<i>Aelurosuchus browni</i>	92	8–?9	?	?
<i>Sesamodontoides pauli</i>	*80–85	8 (lp)	?	?
<i>Bauria cynops</i> (AMNH FARB 5622)	130	11	Incomplete	Absent
<i>Bauria cynops</i> (BP/1/3770) (Brink, 1963: 5th specimen)	117	9	Incomplete	Absent
<i>Bauria cynops</i> (BP/1/1180) (Brink, 1963: 3rd specimen)	114	At least 9	Incomplete	Absent
<i>Bauria cynops</i> (BP/1/2523) (Brink, 1963: 6th specimen)	?	10 (lp)	?	?
<i>Bauria robusta</i>	*132	11	?	?

Postcanine number refers to upper teeth excepts where lp is indicated

\*Inferred

## Discussion

### Taxonomy of Southern African Bauriidae

The bauriids, which include the last therocephalian survivors, are well-represented in the Karoo Basin of South Africa and are also known from Namibia (Keyser 1973a, b; Keyser and Brink 1977–1978), China (Sun 1981, 1991) and Russia (Tatarinov 1973, 1974; Battail and Surkov 2000). The bauriids from southern Africa are small-sized taxa that attain a skull length of up to 133 mm. They can be easily recognized by the characteristic postcanines, as they are the only therocephalian group with buccolingually expanded postcanines (Crompton 1962). In addition, they show an osseous secondary palate comprised of the premaxilla, maxilla, and in some cases, a small contribution of the vomer. Another trait not known in other therocephalians is a maxillary shelf lateral to the tooth row series, a feature which is similar to that of most gomphodont cynodonts (i.e., cynodonts with buccolingually expanded postcanines). In Bauriidae, a similar expansion is also present on the dentary lateral to the lower postcanines and is a clear autapomorphy for the family.

We distinguish two morphotypes of Bauriidae from the CAZ of southern Africa, which represent different species. One morphotype is characterized by an incomplete postorbital bar, absence of parietal/pineal foramen, a large number of postcanines (from eight to 11), and the canine usually located anteriorly in the snout (Table 13.3). This type is herein assigned to the species *Bauria cynops* Broom (1909),

of which we regard *Aelurosuchus browni*, *Baurioides watsoni*, *Microhelodon eumerus*, *Sesamodontoides pauli*, and *Bauria robusta* as synonyms. The inclusion of *A. browni* in this species is based on the anterior placement of the canine and the weak development of the maxillary shelf. *S. pauli* is tentatively included in *B. cynops* based on the postcanine crown that appears to be thin in lateral view. *Microhelodon eumerus* is also tentatively included in this species based on the location of the postcanines near the lateral margin of the maxilla (suggesting little development of the maxillary shelf) and the overall morphology of the preserved postcanines. Other specimens included within this species are shown in Table 13.4. *Bauria robusta* was originally described as being 20 % larger than the largest recognized specimen of *B. cynops* (AMNH FARB 5622); with 11 postcanines, small canines, powerful cheek bulges with deep depressions below and no interpterygoid vacuity. In Brink's (1965) description of the new species, the large size was recognized as the most important trait. Brink (1965, p. 123) noted that the specimen is represented by two-thirds of the skull and that the total preserved skull length is 100 mm. His estimated total skull length of 168 mm appears exaggerated in comparison with our estimation of around 133 mm for this specimen, which is similar to the size of the specimen AMNH FARB 5622. It is clear that size per se is not enough to differentiate this species. Considering the high number of postcanines and the location of the canine well anterior in the snout, we consider this species a junior synonym of *Bauria cynops*. One important character suggesting a difference between *B. robusta* and *B. cynops* was the absence of the interpterygoid vacuity. Further preparation of Brink's holotype indicates that the

**Table 13.4** Geographic distribution of Bauriidae specimens from South Africa

Taxon	Specimen	Locality	District
<i>Microgomphodon oligodens</i>	NHMUK R3305	Near Aliwal North	Aliwal North
	AMNH FARB 5517		Aliwal North
	SAM-PK-5865	Erf 1 Commonage	Aliwal North
	SAM-PK-5866	Erf 1 Commonage	Aliwal North
	BP/1/4655	Hugoskop 620	Rouxville
	SAM-PK-K10160	Lemoenfontein 44	Rouxville
	BSP 1934-VIII-13	Kaaimansgat	Rouxville
	USNM PAL 289115	Matyantya	Cacadu
	USNM PAL 412433 <sup>a</sup>	Matyantya	Cacadu
	USNM PAL 412401 <sup>a</sup>	Matyantya	Cacadu
	NMQR 3189	Eerstegeeluk 131	Bethlehem
	NMQR 3183	Jisreel 419	Harrismith
	NMQR 3596		Wepener
<i>Bauria cynops</i>	SAM-PK-5875	Melkspruit 12	Aliwal North
	BP/1/4678	Betjieskraal 36	Rouxville
	UCMP 4284	Bethel	Rouxville
	RC 114	Lady Frere Area	Cacadu
	BP/1/1180	Matyantya	Cacadu
	USNM PAL 23331	Lady Frere Commonage	Cacadu
	SAM-PK-1333	Vaal Bank 134	Albert
	NHMUK R4095	Essex	Albert
	BP/1/3770	Cragievar	Albert
	BP/1/1685	Grootdam	Albert
	BP/1/1679 <sup>b</sup>	Grootdam	Albert
	AMNH FARB 5622	Winnaarsbaken	Albert
	BP/1/2523	Lady Frere	Albert
	BP/1/2837	Bersheba	Albert
	NHMUK R3581	Near Burgersdorp	Albert

<sup>a</sup> Specimens not observed, they are included here based on comments by Hotton in the museum catalog identifying them as *Sesamodon*

<sup>b</sup> Specimen lost, observed in photos, sketches and notes of Dr Mendrez-Carroll

vacuity is indeed present, however. It is reduced in size relative to that of BP/1/1180, but is similar in size to that of BP/1/3770. This suggests that the tendency toward reduction of the interpterygoid vacuity known in several therocephalians and some cynodonts (e.g., *Thrinaxodon*), appears to also be the case for Bauriidae. It should be mentioned that the interpterygoid vacuity in the large skull AMNH FARB 5622 is described as small by Broom (1937, p. 3) and as large by Boonstra (1938, p. 172), but the vacuity of this specimen is indeed smaller than that of smaller specimens of *B. cynops*.

The second type, herein assigned to *Microgomphodon oligocynus* Seeley (1895), has a complete postorbital bar, a pineal foramen, a small number of postcanines and the canine usually located posteriorly in the snout (Table 13.3). Another important trait is the presence of an extended fossa on the lateral surface of the dentary, in a similar placement as the masseteric fossa in cynodonts. This trait is clearly

represented in SAM-PK-K10160 as well as in GSN R337, but it is absent in BSP 1934-VIII-13. In addition to the new specimen described here, *M. oligocynus* includes all material previously referred to *Sesamodon browni*, *Melinodon simus*, *Watsoniella breviceps*, and *Herpetogale marsupialis*. *Sesamodon browni* is included in this species as it has a complete postorbital bar (Fig. 13.1c), the canine is located posteriorly on the snout, and it has a reduced number of postcanines (Table 13.3). *Melinodon simus* is included based on a posterior keel of the vomer which extends posteriorly almost as far as the base of the pterygoid processes. Several features, including reduced number of postcanines, the posterior location of the canine, placement of the canine well offset from the postcanine series and restricted exposure of the frontal on the dorsal margin of the orbit, allow the inclusion of *W. breviceps* in *M. oligocynus*. NMQR 3189, described by King (1996) as *Bauria* sp., is also included in



**Fig. 13.10** Postcanines of Bauriidae. Stereopair in dorsal view of **a** upper and **b** lower postcanines of *Microgomphodon oligocynus* (BP/1/4655); **c** lateral view of the right upper and lower postcanines

of *Microgomphodon oligocynus* (BMNH R3305); **d** lateral view of the left upper postcanines of *Bauria cynops* (BP/1/1180). Scale 1 cm

*M. oligocynus*, based on the morphology of the postcanines. The postcanine crowns of this taxon have an ovoid outline (Fig. 13.10a, b) with a long curved margin in lateral view, in contrast to the more restricted lateral exposure in the postcanines of *B. cynops* (compare Fig. 13.10c, d).

In addition to the above mentioned features, the Procrustes analysis allowed us to recognize the following additional differences: *M. oligocynus* has a taller but less wide cranium, taller snout, temporal opening more expanded laterally and smaller suborbital vacuity. The mandible of *M. oligocynus* has a higher symphysis, relatively shorter corpus, and more laterally directed coronoid process. It is interesting to note that the snout length, which intuitively appears as a noteworthy difference between these taxa, is not represented in the variations highlighted by the Procrustes analysis. This result is probably related to the

condition of traits in the specimens analysed. The proportion of the length of the snout in relation to the basal cranial length in SAM-PK-K10160 and BP/1/1180 is the closest between representatives of the two different species (Fig. 13.6).

The presence of an ossified interorbital wall between the orbitosphenoid and the palatine in SAM-PK-K10160 is a feature infrequently found in therocephalians and cynodonts. Further preparation of BP/1/1180 enabled recognition of this structure in *Bauria cynops*. This condition was previously reported for whaitsiids from Tanzania (Kemp 1972) and among cynodonts was observed only in a specimen of *Diademodon tetragonus* (BSP 1934-VIII-20). We interpret this lamina as an ossified mesethmoid and the recovery of this delicate feature in both bauriid species indicates that this character is indeed present in the group.

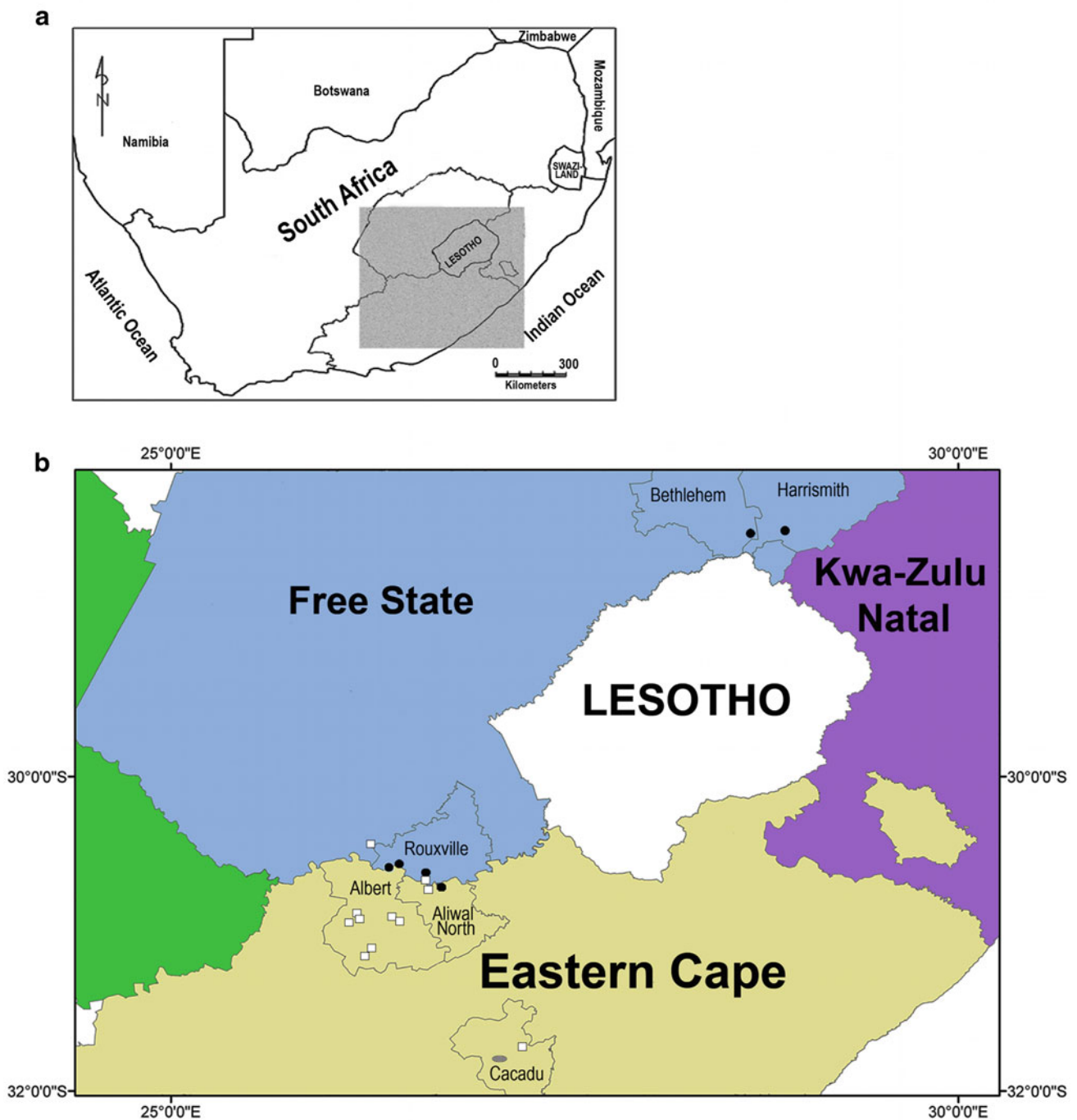


**Fig. 13.11** Distribution of Bauriidae in the South African Karoo. Grey area in (a) is enlarged in (b). Only the districts with bauriid records are represented. Round black, *Microgomphodon oligocynus*; square white *Bauria cynops*; ellipse grey, the two species

### **Temporal and Geographic Distribution of Bauriidae in Southern Africa**

Bauriids from the CAZ are represented by at least 25 specimens and their geographic distribution in the Karoo is restricted to the southwestern part of the basin, with only two exceptions from the northeastern portion (Table 13.4;

Fig. 13.11). In fact, most of the bauriid localities are concentrated in the middle of the Eastern Cape and southern Free State provinces, with the greatest distance between localities being around 150 km.

Three locality clusters have been recognized in the Karoo. The northeastern cluster from outcrops in the Harrismith and Bethlehem districts have produced only

*Microgomphodon oligocynus* (Fig. 13.11), and are from Subzone A (i.e., Olenekian) of the CAZ (Neveling 2004). The other two clusters are in the districts of Rouxville, Albert, and Aliwal North on the one hand, and in the District of Cacadu on the other (Fig. 13.11). A relative abundance of *Bauria cynops* have come from the first of these two clusters, whereas in Cacadu, the locality of Matyantya is the only case in which remains of both species are found together. Most of the outcrops of these two clusters fall within Subzone B (i.e., lower Anisian) of the CAZ. However the two localities recording *M. oligocynus*, Hugokop 620 and Kaaimansgat Rouxville, also have remains of the trirachodontid *Langbergia modisei* (Abdala et al. 2006) and therefore are best interpreted as representing the Subzone A.

The only record in Africa of a CAZ-equivalent bauriid outside of South Africa is from the upper Omingonde Formation at the locality of Rhenosterkloof in Namibia (Abdala and Smith 2009; Keyser and Brink 1977–1978). This is probably the youngest record of Bauriidae (and for that matter of a therocephalian) in Africa, as the specimen was found in the upper Omingonde Formation, near of the contact with the Etjo Formation (Abdala and Smith 2009).

## Conclusions

An exceptionally preserved new specimen (SAM-PK-K10160) of the African bauriid *Microgomphodon oligocynus* provides a new glimpse of morphological features of the species. The presence of a fossa on the lateral surface of the dentary (where it is the masseteric fossa in cynodonts) is a remarkable feature of this species, confirming a previous report by Keyser and Brink (1977–1978) in a specimen from Namibia. Another outstanding feature in the new specimen is a thin ossified wall in the interorbital space, below the orbitosphenoid, that we identified as an ossified mesethmoid.

Our taxonomic revision of Gondwanan bauriids, after examination of nearly all specimens of the group, indicates that two species were represented among southern African bauriids: *Bauria cynops* and *Microgomphodon oligocynus*.

*Microgomphodon oligocynus* is differentiated from *B. cynops* on the basis of clear-cut morphological features such as smaller size (89 vs. ~130 mm of basal skull length in the largest specimens of each species, respectively) and the presence of a complete postorbital bar, pineal foramen, and comparatively large orbits. In addition, *M. oligocynus* features fewer postcanine teeth, with a long curved margin in lateral view, that contrast with the numerous teeth presenting more restricted lateral exposure observed in *B. cynops*.

Further putative differences between these species are provided by a Procrustes analysis of the two best preserved specimens of these species: *M. oligocynus* has a taller but less

wide cranium, taller snout, temporal opening more expanded laterally, and smaller suborbital vacuity. The mandible of *M. oligocynus* has a higher symphysis, relatively short corpus, and more laterally directed coronoid process.

*Microgomphodon oligocynus* appears to have been widely distributed geographically and temporally. In contrast, specimens of *Bauria cynops* are known only from outcrops that are geographically close together (~150 km) and are restricted to the subzone B of the CAZ (probably Anisian-aged). *Microgomphodon oligocynus* is the only species from the northeastern portion of the Karoo Basin and the only African bauriid recorded from Namibia, in both cases from outcrops which are geographically further apart than those of the other representatives of the group. In addition the age range of the latter species appears to be longer than that of *B. cynops*. *Microgomphodon oligocynus* has its earliest occurrence in Subzone A of the CAZ (Late Olenekian) and extends high into the upper Omingonde Formation. Despite the fact that *M. oligocynus* is known from the upper Omingonde Formation, it is important to note that this species has not yet been reported from subzone C of the South African CAZ. This could indicate that subzone C is younger than the upper Omingonde Formation, or that *M. oligocynus* has simply not yet been found at this stratigraphic level in the main Karoo Basin.

**Acknowledgments** We are indebted to the curators of the collections mentioned in this study for access to the material. SAM-PK-K10160 was collected by R. M. H. Smith and Derik Wolvaardt. FA would especially like to thank Sheena Kaal from the Iziko-South African Museum for the loan of SAM-PK-K10160 and extended patience for its delayed return. Preparation of the specimen described and other studied specimens were made by Annelise Crean at the Iziko-South African Museum and A. Nthaopa Ntheri and Charlton Dube at the Bernard Price Institute, Johannesburg. FA is also very grateful to Jim Hopson for access to his notes and figures of bauriids and those of the late Dr. Christiane Mendrez-Carroll. Dr. Oliver Rauhut supplied photos of the type specimen of *Watsoniella*, and Dr. Christian Kammerer provided photos of bauriid specimens from the Smithsonian National Museum of Natural History, U.S. CT-scanning of the specimen was undertaken at the Helen Joseph Hospital (Johannesburg, South Africa) under the guidance of Jaymati Limbachia. We are thankful to Michael Day for his help to provide information for Fig. 13.11 and proofreading. The reviewers of this manuscript, Trond Sirkurdson and Adam Huttenlocker, as well as the editor Christian Kammerer provided important suggestions that improved the final result of this work. The research of FA and BR research was funded by DST, NRF and PAST. TJ's research was supported by the Claude Leon Foundation.

## References

- Abdala, F. (2007). Redescription of *Platycraniellus elegans* (Therapsida, Cynodontia) from the Lower Triassic of South Africa, and the cladistic relationships of Eutheriodontia. *Palaentology*, 50, 591–618.
- Abdala, F., & Smith, R. M. H. (2009). A middle Triassic cynodont fauna from Namibia and its implications for the biogeography of Gondwana. *Journal of Vertebrate Paleontology*, 29, 837–851.

- Abdala, F., Neveling, J., & Welman, J. (2006). A new trirachodontid cynodont from the lower levels of the Burgersdorp Formation (Lower Triassic) of the Beaufort Group, South Africa and the cladistic relationships of Gondwanan gomphodonts. *Zoological Journal of the Linnean Society*, 147, 383–413.
- Battail, B., & Surkov, M. V. (2000). Mammal-like reptiles from Russia. In M. J. Benton, E. N. Kurochkin, M. A. Shishkin, & D. Unwin (Eds.), *The age of dinosaurs in Russia and Mongolia* (pp. 86–119). New York: Cambridge University Press.
- Bookstein, F. L. (1991). *Morphometric tools for landmark data: Geometry and biology*. Cambridge: Cambridge University Press.
- Boonstra, L. D. (1938). On a South African mammal-like reptile, *Bauria cynops*. *Palaeobiologica*, 6, 164–183.
- Botha, J., Abdala, F., & Smith, R. (2007). The oldest cynodont: New clues on the origin and early diversification of the Cynodontia. *Zoological Journal of the Linnean Society*, 149, 477–492.
- Brink, A. S. (1963). On *Bauria cynops* Broom. *Palaeontologia Africana*, 8, 39–56.
- Brink, A. S. (1965). A new large bauriamorph from the Cynognathus-Zone of South Africa. *Palaeontologia Africana*, 9, 123–127.
- Brink, A. S., & Kitching, J. W. (1953). On some new Cynognathus zone specimens. *Palaeontologia Africana*, 1, 29–48.
- Broili, F., & Schröder, J. (1935). Beobachtungen an Wirbeltieren der Karrooformation. VII. Ein neuer Bauriamorphe aus der Cynognathus-zone. *Sitzungsberichte der mathematisch-naturwissenschaftlichen Abteilung der Bayerischen Akademie der Wissenschaften zu München*, 1935, 21–63.
- Broom, R. (1903). On the classification of the theriodonts and their allies. *Report of the South African Association for the Advancement of Science*, 1, 286–294.
- Broom, R. (1905). Preliminary notice of some new fossil reptiles collected by Mr. Alfred Brown at Aliwal North, South Africa. *Records of the Albany Museum*, 1, 269–275.
- Broom, R. (1906). On a new cynodont reptile (*Aelurosuchus browni*). *Transactions of the South African Philosophical Society*, 16, 376–378.
- Broom, R. (1909). Notice of some new South African fossil amphibians and reptiles. *Annals of the South African Museum*, 7, 270–278.
- Broom, R. (1911). On the structure of the skull in cynodont reptiles. *Proceedings of the Zoological Society of London*, 81, 893–925.
- Broom, R. (1913). South African fossil reptiles. *The American Museum Journal*, 13, 334–346.
- Broom, R. (1915). Catalogue of types and figured specimens of fossil vertebrates in the American Museum of Natural History. II.—Permian, Triassic and Jurassic reptiles of South Africa. *Bulletin of the American Museum of Natural History*, 25, 105–164.
- Broom, R. (1925). On some carnivorous therapsids. *Records of the Albany Museum*, 3, 309–326.
- Broom, R. (1931). Notices of some new genera and species of Karroo fossil reptiles. *Records of the Albany Museum*, 4, 161–166.
- Broom, R. (1937). On the palate, occiput and hind foot of *Bauria cynops* Broom. *American Museum Novitates*, 946, 1–6.
- Broom, R. (1950). Some fossil reptiles from the Karroo beds of Lady Frere. *South African Journal of Science*, 47, 86–88.
- Crompton, A. W. (1962). On the dentition and tooth replacement in two bauriamorph reptiles. *Annals of the South African Museum*, 46, 231–255.
- Dryden, I. L., & Mardia, K. V. (1998). *Statistical shape analysis*. London: Wiley.
- Gower, J. C. (1975). Generalized Procrustes analysis. *Psychometrika*, 40, 33–50.
- Haughton, S. H. (1922). On some Upper Beaufort Therapsida. *Transactions of the Royal Society of South Africa*, 10, 299–307.
- Hopson, J. A., & Barghusen, H. R. (1986). An analysis of therapsid relationships. In N. Hotton, P. D. MacLean, J. J. Roth, & E. C. Roth (Eds.), *The ecology and biology of mammal-like reptiles* (pp. 83–106). Washington, DC: Smithsonian Institution Press.
- Huttenlocker, A. (2009). An investigation into the cladistic relationships and monophyly of therocephalian therapsids (Amniota: Synapsida). *Zoological Journal of the Linnean Society*, 157, 865–891.
- Kemp, T. S. (1972). Whaitiid Therocephalia and the origin of cynodonts. *Philosophical Transactions of the Royal Society of London B*, 264, 1–54.
- Keyser, A. W. (1973a). New Triassic vertebrate fauna from south west Africa. *South African Journal of Science*, 69, 113–115.
- Keyser, A. W. (1973b). A new Triassic vertebrate fauna from south west Africa. *Palaeontologia Africana*, 16, 1–15.
- Keyser, A. W., & Brink, A. S. (1977–1978). A new bauriamorph (*Herpetogale marsupialis*) from the Omingonde Formation (Middle Triassic) of South West Africa. *Annals of the Geological Service*, 12, 91–105.
- King, G. (1996). A description of the skeleton of a bauriid therocephalian from the Early Triassic of South Africa. *Annals of the South African Museum*, 104, 379–393.
- Neveling, J. (2004). Stratigraphic and sedimentological investigation of the contact between the *Lystrosaurus* and the *Cynognathus* assemblage zones (Beaufort Group: Karoo Supergroup). *Bulletin of the Council for Geosciences*, 137, 1–165.
- O’Higgins, P., & Jones, N. (2006). Morphologika—tools for statistical shape analysis. York: Hull York Medical School. <http://www.york.ac.uk/res/fme/resources/software.htm>
- Rohlf, F. J., & Slice, D. E. (1990). Extensions of the Procrustes method for the optimal superimposition of landmarks. *Systematic Zoology*, 39, 40–59.
- Seeley, H. G. (1895). Researches on the structure, organization, and classification of the fossil Reptilia. Part IX, Section 4. On the Gomphodontia. *Philosophical Transactions of the Royal Society of London B*, 186, 1–57.
- Sun, A.-L. (1981). Reidentification of *Traversodontoides wangwuensis* Young. *Vertebrata Palasiatica*, 19, 1–4.
- Sun, A.-L. (1991). A review of Chinese therocephalian reptiles. *Vertebrata Palasiatica*, 29, 85–94.
- Tatarinov, L. P. (1973). Cynodonts of Gondwanan habit in the Middle Triassic of the USSR. *Paleontological Journal*, 1973, 200–205.
- Tatarinov, L. P. (1974). Theriodonts of the USSR. *Transactions of the Palaeontological Institute, Academy of Sciences of the USSR*, 143, 1–250.
- van den Heever, J. A. (1994). The cranial anatomy of the early Therocephalia (Amniota: Therapsida). *Annals of the University of Stellenbosch*, 1, 1–59.
- Watson, D. M. S. (1913). On some features of the structure of therocephalian skull. *Annals and Magazine of Natural History*, 8, 65–79.
- Watson, D. M. S. (1914). Notes on some carnivorous therapsids. *Proceedings of the Zoological Society of London*, 1914, 1021–1038.
- Watson, D. M. S. (1921). The bases of classification of the Theriodontia. *Proceedings of the Zoological Society of London*, 1921, 35–98.
- Zollikofer, C. P. E., Ponce De León, M. S., & Martin, R. D. (1998). Computer-assisted paleoanthropology. *Evolutionary Anthropology: Issues, News, and Reviews*, 6, 41–54.